Politecnico di Torino

Automotive Engineering
A.a. 2022/2023
Sessione di Laurea Luglio 2023

Design of a PEMFC system in heavy-duty vehicle application

MATLAB/Simulink environment

Relatori:
Ing. Paolo Guglielmi

Candidati:
Andrea Pandolfo
S278130

Summary

Abstract 4
1. Introduction 5
1.1. Background 5
1.2. Hydrogen Fuel cells applications 6
1.2.1. Hydrogen fuel cells cars 6
1.2.2. Hydrogen Fuel Cell Trucks 12
1.2.3. Hydrogen Fuel Cell Buses 15
1.2.4. Other type of Fuel Cell Electric Vehicle 16
1.3. Hydrogen Fuel cells limitations 20
1.4. Objectives 20
2. State of the art of fuel cell 21
2.1. Fuel cell working principle 21
2.2. Types of fuel cells 22
2.3. Theoretical PEM fuel cell potential and electrical work 25
2.3.1. Effect of temperature and pressure 27
2.4. Fuel cell losses 28
2.4.1. Activation losses 29
2.4.2. Ohmic losses 30
2.4.3. Concentration (or mass transport) losses 30
2.4.4. Fuel crossover losses 31
2.4.5. Polarization curve 31
2.5. Fuel cell operating conditions 32
2.5.1. Operating pressure 33
2.5.2. Operating temperature 34
2.5.3. Reactant flow rates 36
2.5.4. Reactants humidity 38
2.5.5. Fuel cell mass balance 41
2.5.6. Fuel cell energy balance 45
3. Fuel cell system and auxiliaries 47
3.1. Air supply system 49
3.2. Hydrogen supply system 51
3.3. Water management and humidification schemes 51
3.4. Thermal management systems and waste heat recovery (WHR) method 53
3.4.1. Thermal management strategies of PEMFC stacks 54
3.4.2. Waste heat recovery (WHR) 58

3.5. Electrical subsystem 60
4. Vehicle model 63
4.1. Vehicle characteristics 63
4.2. Powertrain description 64
4.2.1. Fuel cell stack 64
4.2.2. Battery pack 65
4.2.3. Electric machine 65
4.2.4. Power electronics 65
4.2.5. Gear transmission 66
5. Simulink model 67
5.1. Vehicle dynamic 68
5.1.1. Driving cycle and longitudinal driver 68
5.1.2. Electric machine 69
5.1.3. Gear transmission 70
5.1.4. Vehicle body 71
5.2. Power supply model 72
5.2.1. Fuel cell stack and Boost DC converter 73
5.2.2. Battery 74
Bibliography 76

Abstract

During the last two decades the interest towards alternative solutions for the propulsion system of automotive vehicles has increasingly grown, in order to face the several environmental problems and the consequent increasingly stringent European regulation. One of the solutions that has been proposed and has risen the biggest scientific interest is the usage of hydrogen fuel cell (more precisely polymeric electrolyte membrane fuel cell, PEMFC). This solution has several advantages:

- PMEFCs are able to convert the chemical energy of the hydrogen into electrical energy exploiting the reverse principle of electrolysis, producing only water and heat, hence without pollutant emissions.
- PEMFCs can operate if there is hydrogen available in the tank, thus the fuel cell electric vehicles have less autonomy issues than battery electric vehicles.
- Hydrogen tank can be refilled in few minutes, unlike the battery electric vehicle that takes a lot of time to recharge the batteries.

The aim of this master thesis is to develop and design the model of a heavy-duty vehicle powered by a hydrogen fuel cell to minimize the energy cost.

Firstly, a general overview of the fuel cell will be presented. Then, the model of the PMFC system will be designed and performed using MATLAB-Simulink.

Generally, the efficiency of a PEMFC is about 0.6. The projected outcome is to increase the efficiency of the system exploiting the heat loss of the fuel cell obtaining a general efficiency of the system of about 0.8.

The PEMFC technology has promising characteristics suitable for the automotive field. Thanks to a proper water management and a thermal management system it may become the best solution for the transportation field. However, the production of the components needed is very niche and then its costs are higher than the technologies currently used. In addition, the supply network for hydrogen fuel is still too narrow and should be improved.

In conclusion, the PEMFC chemical potential and the easily and fast refillable nature of the hydrogen storage system, provided the efficiency of the system is risen and the knowledge on calculations to reach It is deepened, could constitute a greener and cheaper solution for heavy-duty vehicles' sector.

1. Introduction

1.1. Background

For several years by now, different solutions have been investigated both as alternative energy source and alternative fuels, but none of them has been able to replace completely fossil fuels. Between these, particularly, the use of hydrogen as energy source was not much appreciated in the transport and power generation sectors. Nevertheless, in recent times the interest toward the hydrogen is increased, especially from manufacturers of light-duty vehicle and heavy-duty vehicle. This fact is caused also by the new European regulation entered into force in 2020, the so called "Green Deal", setting stricter CO2 performance standards for new passenger cars and vans (new restrictions are expected for heavy-duty vehicles too), to achieve climate neutrality in the EU by 2050, including the intermediate target of an at least 55% net reduction in greenhouse gas emission by 2030 (*CO_2 Emission Performance Standards for Cars and Vans*, n.d.; *Paris Agreement*, 2022-2023). Indeed, the transport sector is responsible for approximately a quarter of the total amount of CO2 emissions in Europe, 70% of which are produced by road transport (Nanaki et al., 2017). Therefore, in this scenario the hydrogen returns to being considered a good solution as alternative fuel for several reasons:

- It is eco-friendly: hydrogen produce only water and heat whether it is used as fuel for internal combustion engine or as fuel for fuel cells vehicle (Schäfer et al., 2006);
- It is the most abundant element on the planet, so it is a lasting solution (Singla et al., 2021);
- It is easy to storage and to transport when it is made liquid, compressing it in high pressure tanks;
- High efficiency: the hydrogen fuel cells efficiency is about 50-60% when they produce only electricity, and it can reach 80-90% when the heat produced is recycled (Shabani & Andrews, 2015);
- Fuel cells vehicle technology allows higher autonomy range and lower refuelling time than battery electric vehicle (Yusuf et al., 2021).

Currently, the main part of the hydrogen is produced via an extraction method which uses natural gas composed by oxygen and hydrogen. This process is cheap, but its greenhouse gas emissions are not zero. However, the so called "green hydrogen", which is the hydrogen produced by means of electrolysis using the electricity produced by renewable energy, can allow to achieve the target of zero emissions of CO2 (Qureshi et al., 2022).

In addition, the several technologies needed for a fuel cells electric vehicle are all already available and tested: indeed, a FCEV uses the same electric motor of a BEV combined with a Fuel Cell (usually in the automotive field the fuel cells used are the Proton-exchange membrane fuel cells, also called polymer electrolyte membrane fuel cells, which are more suitable for their compactness and lower weight) (Selmi et al., 2022; *Toyota Fuel Cell Electric Vehicles | Toyota Europe*, 2022-2023). So, it should be easy both to project new vehicles and to convert older car models into FCEV.

1.2.Hydrogen Fuel cells applications

During the last two decades several companies have shown a considerable interest in the use of fuel cells in the automotive field, mainly in the car and transportation sectors, like buses and trucks. However, recently, fuel cells technologies have been applied also in other segments like agriculture vehicles, construction vehicles, trains, military vehicle and so on. Following some examples of vehicles powered by hydrogen fuel cells belonging to different segments are reported.

1.2.1. Hydrogen fuel cells cars

Although a lot of companies spent time and money working on fuel cell vehicles prototypes, only Toyota, Hyundai and Honda have been able to make a fuel cell vehicle available to retail customers while a new French start-up Hopium presented the prototype of its hydrogen sedan and seems to be ready to launch it on the market. The fuel cell cars are listed below.

Honda FCX Clarity (2008-2014) & Honda Clarity (2016-2021)

The FCX Clarity was the first hydrogen fuel cell vehicle available to retail customers. Its electrical power derives from a 100 kW Honda Vertical Flow hydrogen fuel cell stack whereby electricity is supplied on demand, while the regenerative braking function is ensured by a separate battery used to store the energy. The electric motor used is the same of the EV Plus, which provide 134 hp (100 kW) and a torque of 256 Nm at 0-3056 rpm. The hydrogen tank can store 4,1 kg of hydrogen pressurized at 350 bar and ensure a range of 386 km certified by EPA. The hydrogen averaged consumption is about 100 km per kilogram (*Honda Clarity - Wikipedia*, 2022-2023).

Fig. 1.1 Honda FCX Clarity (2008-2014) (BHD., 2023)

Fig. 1.2 Honda FCX Clarity (2008-2014)- Details (*Review, Jadwal Angsuran, Spek, Gambar, Harga Honda FCX Clarity 2007 | Autofun*, *2022-2023*)

The following generation, the Honda Clarity Fuel Cell, is equipped with an AC permanent-magnet synchronous electric motor able to provide 174 hp (45001-9028 rpm) and a torque of 300 Nm (0-3500 rpm), allowing better performances. The proton exchange membrane fuel cell (PEMFC) ensures an operating range of temperature between -30 C° and 105C° while the fuel cell power output was almost the same. The hydrogen tanks (700 bar) were increased up to 5,46 kg enabling a range of 589 km. Thanks to these improved features the Honda Clarity Fuel Cell had the highest EPA driving range rating of any zero-emissions vehicle in the U.S., until the Hyundai Nexo was released in 2019, with an equivalent fuel consumption equal to 28,9 km/l (*2021 Clarity Fuel Cell Specifications & Features*, 2022-2023; *Honda Clarity - Wikipedia*, 2022-2023).

Fig. 1.3 Honda Clarity (2016-2021) (*Honda Clarity Fuel Cell Vanta Un'autonomia Di 589 Km Certificata EPA*, *2022-2023*)

Despite of the excellent features and performances obtained by the Honda Clarity Fuel Cell, it is not so easy for the fuel cell vehicles to penetrate in the market and, due to the few vehicles sold, Honda stopped the fuel cell vehicles production.

Hopium Alpha 0 (Prototype)

The Alpha 0 is the new sedan presented by Hopium, the new start up belonging to Hydrogen Motive Company. This prototype is powered by a hydrogen fuel cell stack combined with an electric motor which is able to provide above 500 cv (almost 370 kW) and a maximum speed of 230 kmh. However, the best characteristic of this car will be not the speed but the range which will be higher than 1000 km thanks to a storage capability of 10kg of compressed hydrogen at 700 bar (*Hopium, Manufacturer Of High-End Hydrogen Powered Vehicles, Unveils The Hopium Machina Vision and Announces The Opening of Its Order Book - Hydrogen Central*, 2022-2023; *Hopium - Wikipedia*, n.d.; *Hopium Machina Technology*, 2022-2023) .

Fig. 1.4 Hopium Alpha 0 (Prototype) – front view (*Hopium Machina Alpha 0 Hits the Road!*, *2022-2023*)

Fig. 1.5 Hopium Alpha 0 (Prototype) – side view (*La Normandie Ne Veut Pas Perdre Sa Marque Automobile Hopium*, *2022-2023*)

Hyundai ix35 (2013-2018) & Hyundai Nexo (2019-2022)

The Hyundai ix35 FCEV is a hydrogen fuel cell vehicle deriving from the Hyundai Tucson FCEV. The ix 35 FCEV has a more powerful electric engine rated at 100 kW (134 hp) and a range of about 594 km. This improvement is due to the greater hydrogen tanks, which can store 5,64 kg of hydrogen, with

higher storage pressure of 700 bar, as well as fuel technology advances. Indeed, the previous version used a graphite bipolar plate PEMFC which was replaced by a metal bipolar plate PEMFC (*Hyundai Ix35 FCEV - Wikipedia*, 2022-2023; *Hyundai Ix35 Fuel Cell 2013-2018 Review (2023) | Autocar*, 2022-2023).

Fig. 1.6 Hyundai ix35 Fuel Cell (2013-2018) (*Hyundai Ix35 Fuel Cell 2013-2018 Review (2023) | Autocar*, *2022-2023*)

The Hyundai Nexo represents the new generation of FCEV of the south Korean company. Unlike the previous generations, which used a heavily modified version of the Tucson underpinnings, the Nexo has a purpose-built platform from a FCEV standpoint. It has an electric motor which develops 163 cv of power and a torque of 400 Nm. The vehicle is equipped with three hydrogen tanks able to store 6,3 kg of hydrogen ensuring a range between 666 km and 778 km (*Hyundai Nexo - Wikipedia*, 2022-2023; *NEXO | Dimensioni, Prezzo, Listino e Scheda Tecnica | Hyundai*, 2022-2023).

Fig. 1.7 Hyundai Nexo (2019-2022) (*Hyundai Nexo, La Sicurezza Dell'idrogeno - Motori*, *2022-2023*)

Fig. 1.8 Hyundai Nexo (2019-2022)- Details (*Hyundai Goes Full Steam Ahead on Fuel Cell Systems - Electrive.Com*, *2022-2023*)

Toyota Mirai II (2020-2022)

The Toyota Mirai is a mid-size hydrogen fuel cell vehicle manufactured by Toyota and is one of the first fuel cell vehicle to be mass-produced and sold commercially. It uses both the hybrid technology of the Hybrid Sinergy Drive and the fuel cell technology. The first model was already considered the most fuel-efficient hydrogen fuel cell vehicle rated ate the time by EPA with the MPG-equivalent combined city/highway fuel economy rating equal to 66mpg_us (3,6 l/100 km) and a range of 502 km (Toyota, 2014; *Toyota Mirai - Wikipedia*, 2022-2023).

Fig. 1.9 Toyota Mirai (2014-2019) (*Toyota Mirai Hydrogen Fuel Cell*, n.d.)

The second generation, the Toyota Mirai II, set a world record of travelling 1360 km with a full tank of 5,65 kg hydrogen. This great achievement is due both to the new Toyota's modular GA-L platform, which can accommodate a more efficient FCEV powertrain and greater hydrogen tanks thanks to a better space distribution, and the renewed fuel cell, whose specific power density have been increased allowing a higher power than the previous model with a smaller fuel cell stack containing less cells (330 instead of 370). The improvement of all the components allowed to increase the power of 12% reducing the weight of 42%. Moreover, the performance of the vehicle at low temperature have been improved and the vehicle can start also at -30° (*2023 Toyota Mirai | Toyota.Com*, 2022-2023; *LCA | 2nd Generation Toyota Mirai | Toyota Europe*, 2022-2023; *Toyota Mirai - Wikipedia*, 2022-2023).

Fig. 1.10 Toyota Mirai II (2020-2022) (*LCA | 2nd Generation Toyota Mirai | Toyota Europe*, *2022-2023*)

Fig. 1.11 Toyota Mirai II (2020-2022)- Details (*New Mirai Hydrogen Fuel Cell Electric Vehicle - under the Skin - Toyota UK Magazine*, *2022-2023*)

Table 1- FC Car Technical Specifications

FC CAR	FC Power	E-Motor Type	E-Motor Power	Max Torque	Hydrogen Storage Capability	Autonomy Range	Equivalent Fuel Consumption
Honda Clarity	PEMFC (>100kW)	P-M Synchronous	130 kW	300 Nm	5,46 kg	589 km	28.9 kml
Hyundai ix35	PEMFC (Metal bipolar plate)	Induction motor	100 kW	300 Nm	5.64 kg	594 km	27.8 kml
Hyundai NEXO	PEMFC (95 kW)	P-M Synchronous	120 kW	400 Nm	6.3 kg	666-778 km	26.1 kml
Toyota Mirai II	PEMFC (128 kW)	P-M Synchronous	134 kW	300 Nm	5,6 kg	1360 km	31.5 kml
Hopium Alpha 0	-	-	370 kW	-	10 kg-	>1000 km	-

1.2.2. Hydrogen Fuel Cell Trucks

The heavy-duty transportation sector is probably the most appropriate for the use of fuel cell vehicles. Indeed, unlike the passenger car sector, the heavy-duty transport sector has low manufacturing volumes (so the cost difference with the ICE is reduced). In addition, the fuel cell vehicle characteristics such as long range and short time required for refuelling match perfectly the heavy-duty transportation needs (Staffell et al., 2019). Furthermore, the trucks have more space to accommodate the fuel cell stacks and the hydrogen tanks and the weight issue of the fuel cell is less important since most of the weight is due to the cargo.

For what concern this segment, three are the company that have shown increased interest and are stepping forward into the new business of the hydrogen mobility: Hyundai, with the XCIENT Fuel Cell, Iveco (CNH Industrial), which in collaboration with Nikola presented the Nikola 3, and Daimler Truck of the Mercedes-Benz Group which is working on a new prototype Mercedes -Benz GenH2.

Hyundai XCIENT Fuel Cell

The Hyundai Xcient fuel cell is a hydrogen fuel cell powered 34-ton cargo truck derived by the Hyundai Xcient thanks to the joint venture with Swiss company H2 Energy. XCIENT is powered by a 190-kW hydrogen fuel cell system with dual 95- kW fuel cell stacks. The battery is a 661 V/ 73.2 kWh lithium battery by Akasol. The electric motor made by Siemens has a rated power of 350 kW and a torque of 3400 Nm. Seven large hydrogen tanks with a filling pressure of 350 bar offer a combined storage capacity of around 32.09 kg of hydrogen. The driving range is about 400 km on a single refuelling and the refuelling time is approximately 8-20 minutes, while the maximum speed of 85 kmh (Hyundai, 2022; *Hyundai Fuel Cell Truck & Bus | Hydrogen-Powered, Zero-Emission Car*, 2022-2023).

Fig. 1.12 Hyundai Xcient Fuel Cell Truck (*XCIENT Fuel Cell | HYUNDAI Truck & Bus*, *2022-2023*)

CNH Nikola 3 Fuel Cell

The Nikola 3 is based on the car body of the Iveco S-Way while the Nikola Motor's technologies are used both for the electric powertrain and the infotainment. The fuel cell version will be able to reach 1000km range. The Nikola 3 electric motor has a rated power of 480 kW and a peak torque of 1800 Nm. The max achievable speed is 121 kmh. The hydrogen tanks will be able to store 80 kg of compressed hydrogen at 700 bar and the refuelling time will be about 15 minutes (*CNH Industrial's Iveco Unveils First Electric Truck in Partnership with Nikola | Reuters*, 2022-2023; *Nikola to Utilize Fuel-Cell Power Modules Using Technology Licensed from Bosch - Green Car Congress*, 2022-2023; *Tre FCEV: Fuel-Cell Electric Metro-Regional Semi-Truck*, 2022-2023).

Fig. 1.13 Nikola 3 Fuel Cell Truck (by Iveco) (*Iveco Presents New BEV & FCEV Vans and Trucks with Hyundai & Nikola Motor - Electrive.Com*, *2022-2023*)

Mercedes-Benz GenH2

The new hydrogen fuel cell concept truck is envisioned for flexible and demanding long-haul transport. It is expected to have a range of up to 1000 km using two tanks able to store 40 kg of liquid hydrogen each (80 kg total). The hydrogen fuel cell system of 300 kW (2x 150 kW) is flanked by a 70-kWh battery pack with a power output of up to 400 kW to support two electric motors of 330 kW each (*Daimler Plans H2 Truck with 1,000 Km Range - Electrive.Com*, 2022-2023; *Development Milestone: Daimler Truck Tests Fuel-Cell Truck with Liquid Hydrogen - Daimler Truck Media Site*, 2022-2023; *Fuel-Cell Mercedes-Benz GenH2 Truck Passes Challenging Tests With Flying Colors - Autoevolution*, 2022-2023).

Fig. 1.14 Mercedes-Benz GenH2 Fuel Cell Truck (*Daimler and Shell Team up on Hydrogen Trucks*, *2022-2023*)

Table 2- FC Truck Technical Specifications

FC Truck	FC Stack	E-M Power	E-M Torque	Hydrogen Storage Capability	Autonomy Range
Hyundai Xcient	PEMFC (2 x 95 kW)	350 kW	3400 Nm	32.09 kg	400 km
CNH Nikola 3	PEMFC (200-300 kW)	480 kW	1800-2700 Nm	80 kg	500-1000 km
Mercedes-Benz GenH2	PEMFC (2 x 150 kW)	2 x 330 kW	1577-2071 Nm	80 kg	1000 km

1.2.3. Hydrogen Fuel Cell Buses

The application of fuel cells for vehicle for the collective transport of people on urban and suburban routes is of particular interest, especially for large cities where pollution is to be limited (*Fuel Cell Bus - Wikipedia*, 2022-2023).

Fig. 1.15 Toyota Sora- Fuel Cell bus (*Toyota Ramps up Efforts to Look at Potential of Hydrogen Vehicles*, *2022-2023*)

An example of Hydrogen fuel cell bus is the Toyota Sora, produced by Toyota and developed in cooperation with Hino Motors. The vehicle is equipped with components originally developed for the Toyota Mirai. The Sora uses two sets of polymer electrolyte fuel cells powering two electric motors with a power output of 155 cv. The bus is provided with a power system that can be used as an emergency source of electricity, providing external consumers with up to 235 kWh of electricity with a maximum power of 9 kW (*TOYOTA PRESENTA IL PROTOTIPO "SORA", L'AUTOBUS EQUIPAGGIATO CON CELLE A COMBUSTIBILE*, 2022-2023; *Toyota Sora - Wikipedia*, 2022-2023; *Toyota Sora Fuel Cell Bus Gets More Safety and Communication Tech - Autodevot*, 2022-2023).

Fig. 1.16 Toyota Sora- Fuel Cell bus-Details (*Toyota Fuel Cell Applications | Toyota Europe*, n.d.)

1.2.4. Other type of Fuel Cell Electric Vehicle

The automotive and transport sector are not the only ones in which the use of hydrogen fuel cell has been tested.

In the railway sector on-board hydrogen fuel is used as source of energy to power traction motors, or the auxiliaries, or both. This kind of train are generally called hydrail. Hydrail vehicles use the chemical energy of hydrogen for propulsion, either by burning hydrogen in a hydrogen internal combustion engine, or by reacting hydrogen with oxygen in a fuel cell to run electric motors. Hydrail vehicles are usually hybrid vehicles with renewable energy storage, as batteries or super capacitors, for regenerative braking, improving efficiency and lowering the amount of hydrogen storage required (*Hydrail - Wikipedia*, 2022-2023).

Fig. 1.17 Alstom-Coradia iLint-Hydrail (*Alstom's Coradia ILint Hydrogen Train Runs for the First Time in France | Alstom*, n.d.)

The Coradia iLint is the world's first passenger train powered by a hydrogen fuel cell, which produces electrical traction. The iLint combines different innovative elements such as clean energy, conversion, flexible energy storage in batteries, and smart management of traction power and available energy. It is specifically designed to non-or partially electrified lines and enables clean, sustainable train operation while ensuring high levels of performance. The train is emission-free and low-noise. It has a range of 1000 km on a single tank of hydrogen. Just 1kg of hydrogen can do the same as around 4.5 kilos of diesel. The train can go at a maximum speed of 140 kmh, much more than regular speeds needed on the line (between 80-120 kmh) (*Alstom's Coradia ILint Hydrogen Train Runs for the First Time in France | Alstom*, n.d.; *Alstom Coradia-LINT - Wikipedia*, 2022-2023; *Alstom Coradia ILint*, 2022-2023.; *Alstom Unveils Hydrogen Fuel Cell Regional Train Coradia ILint - Green Car Congress*, 2022-2023).

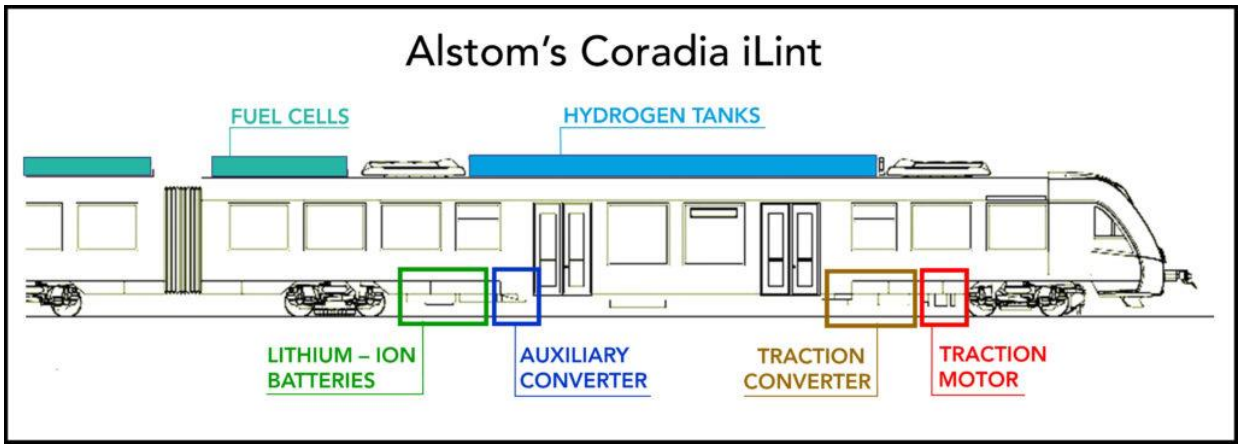

Fig. 1.18 Alstom's Coradia iLint-details (*Hydrogen Trains Coming Soon? - Rail Engineer*, n.d.)

In the agriculture sector as well the fuel cell applications can bring great benefits. Indeed, employing Hydrogen FCEV and investing in renewable energy source which can be used for the hydrogen production through electrolysis, it should be possible to achieve the total energy independence for a farm (*New Holland's NH2 Hydrogen Fuel Cell Tractor*, 2022-2023).

Fig. 1.19 New Holland Agriculture NH2-Hydrogen tractor (*Hydrogen-Fuelled Tractors: A Clean Energy Option for Farmers*, n.d.)

For this objective, it was devised by New Holland Agriculture the new hydrogen tractor NH2. The tractor three fuel cell stacks developing 100kW of power. It mounts two electric motors, one for traction and one for the auxiliaries. Each of the electric motors has a power output of 100 kW, with continuous torque of 950 Nm and a maximum torque of 1200 Nm, with the efficiency at maximum power output equal to 96% and a top speed equal to 50 kmh. The Hydrogen tank can store 8.2 kg of hydrogen at a pressure of 350 bar enabling an operating time up to 3 hours (*New Holland Presents the First NH2^{TM} Hydrogen Powered Tractor Ready to Go into Service on a Farm | NHAG*, 2022/2023).

Fig. 0.1 New Holland Agriculture NH2-Hydrogen tractor-Details (*New Holland NH2 Hydrogen Tractor | Inhabitat - Green Design, Innovation, Architecture, Green Building*, 2022/2023)

For what concerns the construction sector the UK company JCB presented the first hydrogen 20-ton excavator called 220X, but they have not published any technical characteristic (*JCB's First Hydrogen Powered Excavator | News | JCB.Com*, 2022/2023).

Fig. 0.2 JCB 220X- hydrogen excavator (*JCB's First Hydrogen Powered Excavator | News | JCB.Com*, n.d.)

Finally, the hydrogen fuel cell has been tested also on military vehicles. For instance, the USA army began experimentation on a new pick up, the Chevrolet Colorado ZH2. Indeed, the low-noise characteristic together with the long range, the low refuelling time, and the possibility to be used as an electric generator can be precious features in field missions (*Engineering the Extreme Capability of the Colorado ZH2*, n.d.; *Mission-Ready Chevrolet Colorado ZH2 Fuel Cell Vehicle Breaks Cover at U.S. Army Show*, 2022/2023).

Fig. 0.3 Chevrolet Colorado ZH2- first military vehicle powered by hydrogen fuel cells (*About the Fuel Cell Power Chevy Colorado ZH2| Wright Chevy Buick GMC*, 2022/2023)

1.3.Hydrogen Fuel cells limitations

Despite the many advantages due to the usage of hydrogen fuel cell vehicle there are some problems that cannot allow its total market penetration: high selling prices, supply network to be built entirely, relatively high cost of production of the hydrogen (DeCicco, 2004; Kramer, 2017), and furthermore, it is not energetically convenient (unless renewable energy resources are used), because the energy amount required for the hydrogen production is more than the amount of energy stored in the hydrogen itself (*Executive Summary – Global Hydrogen Review 2022 – Analysis - IEA*, 2022/2023). However, some companies by collaborating, like Hyundai and the Swiss company H2 Energy, are investing in the hydrogen business trying to grow both the demand, for instance with the commercial transport service, and the supply building new hydrogen refuelling station (*» Hyundai e H2Energy Insieme per Una Spinta Alla Mobilità Idrogeno in Europa*, n.d.; *Hyundai e H2 Energy: Nuova Joint Venture per Spingere La Mobilità a Idrogeno in Europa*, 2022/2023).

1.4.Objectives

The aim of this master thesis is to develop the model of a PEMFC powertrain system of a heavy-duty vehicle powered by hydrogen fuel cell in order to analyse its potential. As first, a brief explanation of how polymeric membrane fuel cells work will be reported together with the basic equation needed for the thermal model. Then, the model and the management strategy will be discussed. Eventually, the results of the energy management of the vehicle and the conclusions will be argued.

2. State of the art of fuel cell

2.1.Fuel cell working principle

A fuel cells are devices which are able to produce electrical energy from the chemical energy of reactants through electrochemical reaction, promising power generation with high efficiency and low environmental impact. Unlike the internal combustion engines which exploit the combustion to produce energy, the fuel cells are not limited by thermodynamic limitation of heat engines such as the Carnot efficiency. Moreover, avoiding combustion, fuel cells produce power with minimal (or null) pollutant emission. The fuel cells exploit the reverse principle of electrolysis, conveying the electrons produced by the hydrogen oxidation through an electric circuit (Barbir, 2012; Sharma & Pandey, 2021). They can be used in both stationary and mobile applications.

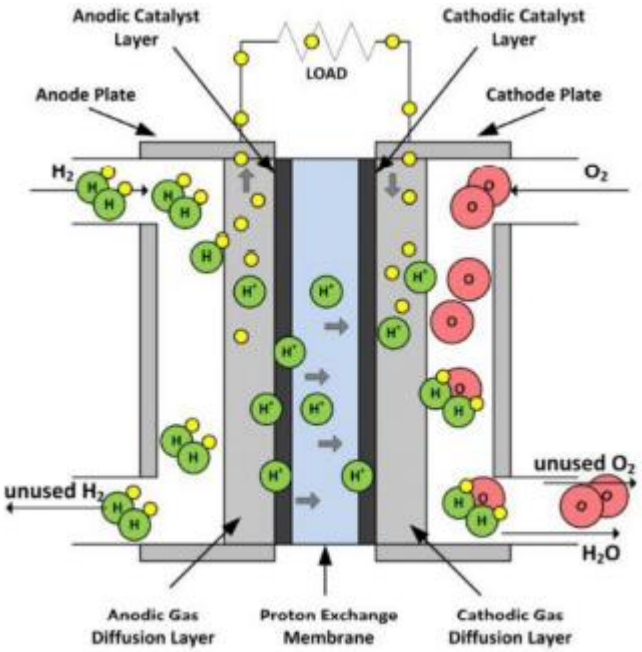

Fig. 2.1 Schematic representation of PEM fuel cell (Sharma & Pandey, 2021)

A fuel cell unit is made up of following components: anode and cathode catalyst layer, bipolar plate, gas diffusion layer and electrolyte (membrane). The hydrogen is fed into the anode gas channel of the bipolar plate, then it passes through the gas diffusion layer and reaches the catalytic reaction site. Here the oxidation reaction take place producing electrons and hydrogen ions:

$$H_2 \rightarrow 2H^+ + 2e^-$$

Eq. 1

After that, the hydrogen ions (protons) are allowed to pass through the membrane, while the electrons are forced to pass through an external circuit, creating current flow and thus producing electrical energy for the load linked to the circuit. At the cathode side oxygen (which can be pure oxygen o air) is fed in the cathode gas channel and reaches the catalyst layer after crossing the gas diffusion layer. In the cathode catalyst layer, the reduction reaction take place:

$$\frac{1}{2}\,O_2 \;+\; 2H^+ + 2e^- \rightarrow H_2O$$

Eq. 2

Therefore, combining the two reactions which occur separately in the two electrodes, the overall reaction is obtained:

$$H_2 + \frac{1}{2}O_2 = H_2O$$

Eq. 3

The only products of the overall reaction are water and heat. In addition, it is important to notice that the reactions just mentioned are global reactions, and in both anode and cathode catalyst layer there are a lot of intermediary steps to reach the final form.

Fuel cell technologies are characterized by some interesting features:

- They have a high electrical efficiency (up to ≈ 0.6) and the overall efficiency of the system could reach also greater values applying proper thermal management and water management of the stack. These results are considerably better than the efficiency achievable with internal combustion engines.
- They have a good operating range with high level of efficiency.
- They can use several types of fuel as reactants (hydrogen, methanol, methane, etc…).
- Their environmental impact is limited.
- They can be used for co-generation (can produce both power and heat).

2.2.Types of fuel cells

Fuel cells can be grouped by the type of the electrolyte employed. These fuel cell types have different fields of application depending on their several features (range of operating temperature, poisoning sensitivity, start-up time, etc…). In this section will be shown an overview of the six major groups of fuel cells.

Alkaline fuel cells (AFCs)

AFCs use concentrated alkaline solution of potassium hydroxide (KOH 85 wt%) as the electrolyte for high -temperature operation (250 C°) and less concentrated (KOH 35-50 wt%) for low-temperature fuel cells (<120 c°). In this type of fuel cells the electrolyte is retained in a matrix, and a wide range of electrocatalyst ca be used (Ni, Ag, metal oxides, noble metals...) (Barbir, 2012). The electrolyte carries a hydroxide ion (OH^-). The reactions that occur at the electrodes are:

Anode: $2H_2 + 4OH^- \rightarrow 4H_2O + 4e^-$

Eq. 4

Cathode: $\frac{1}{2}O_2 + 4e^- + 2H_2O \rightarrow 4OH^-$

Eq. 5

It is important to note that in this case water formation occurs at the anode side, while in the cathode one the water is requested to reduce the oxygen. Therefore, the water management becomes difficult and sometimes waterproof electrodes are used to keep the water into the electrolyte. AFC efficiency can reach maximum values around 70% thanks to their fast kinetics due to low activation losses. Moreover, the oxygen the oxygen reduction reaction (ORR) kinetics at the cathode are simpler than in acidic cells due to inner alkaline solution characteristics. So, it is possible to use cheaper catalyst metals. Nevertheless, the electrolyte is sensitive to carbon dioxide poisoning. For this reason, AFCs need pure hydrogen and pure oxygen to be fed.

Phosphoric acid fuel cells (PAFCs)

These fuel cells use highly concentrated or pure liquid phosphoric acid (H_3PO_4) saturated in silicon carbide (SiC) matrix as electrolyte for ions conduction. Platinum is used as electrocatalyst in both anode and cathode catalyst layer. The half reaction occurring in the respective electrode are:

Anode: $2H_{2(g)} \rightarrow 4H^+ + 4e^-$

Eq. 6

Cathode: $O_{2(g)} + 4H^+ + 4e^- \rightarrow 2H_2O$

Eq. 7

Their maximum efficiency achievable is about 70% and their operating range is 150-200 C°. The freezing point of the phosphoric acid is 42 C°, and so its temperature must be kept above this limit. If these fuel cells are used for intermittent operations, they must be heated every time they are started and then this thermal energy is lost when the cells are switched off. Generally, this type of cells is suitable for co-generation and can be fed with different fuels.

Molten carbonate fuel cells (MCFCs)

These cells use molten carbonate salt mixture suspended in a porous, chemical inert ceramic matrix of beta-alumina solid electrolyte. They operate at relatively high temperatures, around 500-800 C°. MCFC's efficiency can achieve values of about 0.6 and 0.85 with co-generation. Instead of using pure hydrogen, they can use hydrogen bounded fuels which are converted into hydrogen by internal reforming.

The half reactions are:

Anode: $H_2 + CO_3^{2-} \rightarrow H_2O + CO_2 + 2e^-$

Eq. 8

Cathode: $\frac{1}{2}O_2 + CO_2 + 2e^- \rightarrow CO_3^{2-}$

Eq. 9

Internal reformer: $CH_4 + H_2O \rightarrow 3H_2 + CO$

Eq. 10

It can be noticed that the half-reactions of these cells are quite different with respect to the other fuel cell types. Carbon dioxide must be provided at the cathode, but it can be recycled from the anode. Because of their high operating temperature MCFCs are generally used in stationary applications. Moreover, the high temperatures enable the decomposition of hydrocarbons into hydrogen and speeds up the reaction kinetics allowing the usage of cheap catalyst. However, higher temperature causes a faster component breakdown and dangerous corrosion issues for the electrodes.

Solid oxide fuel cell (SOFCs)

SOFCs use oxide or ceramic electrolyte (Y_2O_3 or ZrO_2) as electrolytes. Instead of conducting positive ions as in the other fuel cells, SOFCs electrolyte conducts negative oxygen ions. The reactions occurring at SOFC anode and cathode are respectively:

Anode: $H_2 + O^2 \rightarrow H_2O + 2e^-$

Eq. 11

Cathode: $\frac{1}{2}O_2 + 2e^- \rightarrow O^{2-}$

Eq. 12

They are characterized by extremely high temperature range (700-1200 C°). This working condition leads to some issues such as prolonged start-up time needed, proper material choice both from a thermal and a chemical point of view. However, high operating temperature allows the SOFC to have some good characteristics such as (Bonci, 2021):

- Fuel flexibility: light hydrocarbon fuel can be internally reformed, avoiding the pure hydrogen.
- Reduced activation losses and so improved kinetics of oxygen ions transport.
- Cheap catalyst can be used. Therefore, this type of fuel cell has relatively low cost.
- High co-generation efficiency.

Direct methanol fuel cell (DMFCs)

DMFCs working principle is about the same of the PEMFC, but in this case the fuel cell is fed with methanol instead of hydrogen. Indeed, methanol is easier to store, distribute and sell than hydrogen. Moreover, methanol is simple and cheap to produce on large scale from fossil fuels and can be obtained from agriculture products. This type of cells works in a low range of temperature (70-120 C°) and has the lowest efficiency level with respect to the other fuel cell types (30-40%). The reason

way its efficiency is so low is the methanol cross-over through the membrane, which is the main drawback of this technology.

The half-cell reactions are:

$$\text{Anode: } CH_3OH + H_2O \rightarrow 6H^+ + 6e^- + CO_2$$

Eq. 13

$$\text{Cathode: } \frac{3}{2}O_2 + 2H^+ + 2e^- \rightarrow H_2O$$

Eq. 14

Proton exchange membrane fuel cell (PEMFCs)

PEMFCs are also known as *polymer electrolyte membrane fuel cell* and exploit the reverse principle of the electrolysis. The electrolyte in these cells is a solid polymer membrane made of perfluoro sulfonic acid also named as NAFION (Barbir, 2012; Sharma & Pandey, 2021). The hydrogen positive ions are transported from the anode through the membrane to the cathode. The temperature range is quite low (60-105 C°) and their maximum efficiency is about 0.6-0.65. Due to the slow reaction kinetics platinum must be used as catalyst to reduce the activation losses. This type of fuel cell must be fed with pure hydrogen at the anode, while at the cathode side can be used either pure oxygen or air (most common). Water management and thermal management are fundamental to avoid the membrane drying out too much, affecting the correct operating condition. PEMFCs are the best solution for automotive field because of both their high power-density, low temperature usage, which enable a fast start-up and low risk of corrosion. The reactions in the electrodes are:

$$\text{Anode: } H_2 \rightarrow 2H^+ + 2e^-$$

Eq. 15

$$\text{Cathode: } \frac{1}{2}O_2 + 2H^+ + 2e^- \rightarrow H_2O$$

Eq. 16

$$\text{Overall reaction: } H_2 + \frac{1}{2}O_2 \rightarrow H_2O$$

Eq. 17

2.3.Theoretical PEM fuel cell potential and electrical work

Considering a PEM fuel cell fed with hydrogen, the overall reaction is the same as the reaction of the hydrogen combustion, which is an exothermic process. Therefore, the total amount of energy of the overall reaction is the difference between the heats of formation of products and reactants, which is equal to (Barbir, 2012; Liso & Araya, 2021):

$$\Delta H = (h_f)_{H_2O} - (h_f)_{H_2} - \frac{1}{2}(h_f)_{O_2} = -286\ kJmol^{-1}$$

Eq. 18

This equation is valid only if the enthalpy of formation of both reactants and products are considered at 25C° and at atmospheric pressure.

However, in every chemical reaction some entropy is produced, and because of that part of the enthalpy of the reaction will be lost. Indeed, the theoretical amount of energy that can be exploited is equal to the Gibbs free energy, which is equal to:

$$\Delta G = \Delta H - T\Delta S$$

Eq. 19

Where ΔS is the entropy produced by the reaction, which is equal to:

$$\Delta S = (s_f)_{H_2O} - (s_f)_{H_2} - \frac{1}{2}(s_f)_{O_2}$$

Eq. 20

Then the maximum amount of electrical energy generated in a fuel cell corresponds to the Gibbs free energy, ΔG.

$$\mathrm{W_{el}} = -\Delta G$$

Eq. 21

Considering that the electrical work can be computed as follows:

$$W_{el} = nFE$$

Eq. 22

Where n is the number of electrons per molecule and F is the Faraday's constant. The theoretical fuel cell potential is then:

$$E_{cell} = -\frac{\Delta G}{nF} = -\left(\frac{\Delta H}{nF} - \frac{T\Delta S}{nF}\right)$$

Eq. 23

At 25 C°, the theoretical hydrogen/oxygen fuel cell potential is $E = 1.23$ Volts.

Being the efficiency of any energy conversion the ratio between useful energy output and energy input, the maximum theoretical efficiency of a PEM fuel cell is:

$$\eta = \frac{-\Delta G}{-\Delta H}$$

Eq. 24

And if both numerator and denominator are divided by nF the fuel cell efficiency may be expressed as a ratio of two potential:

$$\eta = \frac{-\frac{\Delta G}{nF}}{-\frac{\Delta H}{nF}} = \frac{E_{cell}}{1.482}$$

Eq. 25

Where the numerator and the denominator represent respectively the theoretical fuel cell voltage and the potential corresponding to hydrogen's higher heating value, which is the thermoneutral potential.

2.3.1. Effect of temperature and pressure

As shown in Eq. 23 the theoretical fuel cell potential changes with temperature. Furthermore, both ΔH and ΔS are functions of temperature (Barbir, 2012):

$$h_T = h_{298,15} + \int_{298,15}^{T} c_p dT$$

Eq. 26

$$s_T = s_{298,15} + \int_{298,15}^{T} \frac{1}{T} c_p dT$$

Eq. 27

Considering that also the specific heat is function of temperature, the following empirical relationship can be used:

$$c_p = a + bT + cT^2$$

Eq. 28

Where a, b, c are the empirical coefficients, different for each gas, codified such as in XXX

Then, substituting the Eq. 28 into both the Eq. 26 and Eq. 27 and integrating, ΔH_T and ΔS_T can be found.

Effect of pressure

All the previous equations are valid at atmospheric pressure. However, generally a fuel cell may operate at pressure that ranging from atmospheric pressure up to 7 bar. For an isothermal process, considering the species involved as ideal gases, the change in Gibbs free energy due to the pressure variation is (Barbir, 2012):

$$dG = RT\frac{dP}{P}$$

Eq. 29

And after the integration:

$$G = G_0 + RT \ln\left(\frac{P}{P_0}\right)$$

Eq. 30

Where G_0 is the Gibbs free energy at standard temperature and pressure (25 C° and 1 atm), and P_0 is the standard pressure (1 atm).

Considering that the change in Gibbs free energy for any reaction is the difference between the Gibbs free energy of the products and the reactants one, it can be computed as following(Barbir, 2012):

$$\Delta G = \Delta G_0 + RT \ln\left[\frac{\left(\frac{P_C}{P_0}\right)^m \left(\frac{P_D}{P_0}\right)^n}{\left(\frac{P_A}{P_0}\right)^j \left(\frac{P_B}{P_0}\right)^k}\right]$$

Eq. 31

This is the Nernst equation and for the hydrogen/oxygen fuel cell reaction becomes:

$$\Delta G = \Delta G_0 + RT \ln\left[\frac{P_{H_2O}}{P_{H_2} P_{O_2}^{0.5}}\right]$$

Eq. 32

By introducing the Eq. 23 in Eq. 32 the cell potential is given by:

$$E = E_0 + \frac{RT}{nF} \ln\left(\frac{P_{H_2} P_{O_2}^{0.5}}{P_{H_2O}}\right)$$

Eq. 33

Furthermore, if the reactants are diluted (which is the case when the fuel cell cathode is fed with air instead of pure oxygen) their partial pressure is proportional to their concentration, so the cell potential is lower. The theoretical voltage loss in case of air is used is equal to (Barbir, 2012):

$$\Delta E = E_{O_2} - E_{air} = \frac{RT}{nF} \ln\left(\frac{P_{O_2}}{P_{air}}\right)^{0.5} = \frac{RT}{nF} \ln\left(\frac{1}{0.21}\right)^{0.5}$$

Eq. 34

2.4.Fuel cell losses

As shown before, also if a fuel cell is not subject to a current flow, so, if its electrical circuit is kept open, the resulting open circuit voltage (OCV) will be lower than the theoretical cell voltage due to the actual operating conditions (such as temperature, pressure, reactants concentration). Besides this energy loss, when the circuit is closed and current flow through the fuel cell, it is always subject to other energy losses which can be divided into 4 categories: activation losses, ohmic losses, concentration (or mass transport) losses and crossover losses.

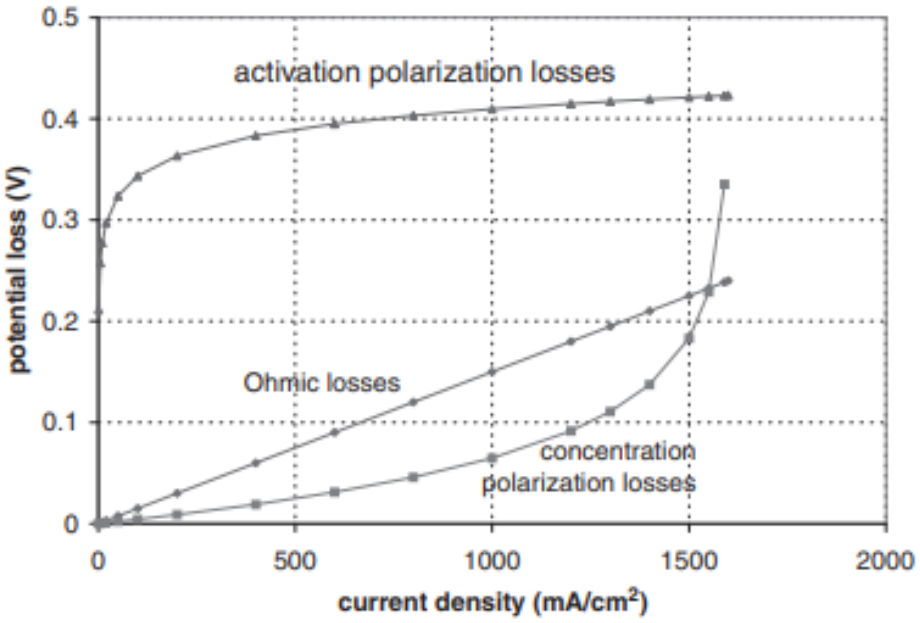

Fig. 2.2 PEM fuel cell losses (Barbir, 2012)

2.4.1. Activation losses

These losses are related to the slow kinetics of the electrochemical reaction at the surface of electrodes. They are called activation losses because they are due to the voltage difference in electrodes, which is needed to start the reaction. These losses happen at both anode and cathode and their expressions comes from the Butler-Volmer equations of the respective electrodes (Barbir, 2012; Usmanov, 2022).

At relatively high negative overpotentials (i.e., potentials lower than the equilibrium potential) such as those at fuel cell cathode, the activation losses at the cathode can be expressed as:

$$\Delta V_{act,c} = E_{r,c} - E_c = \frac{RT}{\alpha_c nF} \ln\left(\frac{i}{i_{0,c}}\right)$$

Eq. 35

Where R is the universal gas constant; F is the Faraday constant; T is the temperature, α is the transfer coefficient; n is the number of moles; i is the current density of the fuel cell and i_0 the exchange current density.

Similarly, at positive overpotential, as it happens in the anode, the activation losses are:

$$\Delta V_{act,a} = E_a - E_{r,a} = \frac{RT}{\alpha_a nF} \ln\left(\frac{i}{i_{0,a}}\right)$$

Eq. 36

It is important to notice that, having different reactions at the cathode and at the anode sides, the transfer coefficient and the exchange current density are different. Indeed, the activation losses of the hydrogen oxidation reaction is much smaller than the activation voltage drop due to oxygen

reduction reaction. Then, if the anode activation losses are neglected, the activation losses can be simplified as:

$$\Delta V_{act} = \frac{RT}{\alpha n F} \ln\left(\frac{i}{i_0}\right)$$

Eq. 37

It can be useful to notice that these losses are predominant at low current densities and the higher is the exchange current density, the lower will be the activation losses. It is possible to reduce the activation losses through the following actions (Barbir, 2012; Bonci, 2021):

- Increasing the fuel cell temperature
- Improving the effectiveness of the catalyst
- Increasing the reactants concentrations
- Using electrodes with higher roughness

2.4.2. Ohmic losses

Ohmic losses are given by the resistance to the flow of ions in the electrolyte and the resistance to the flow of electrons through the electrically conductive fuel cell components: gas diffusion layer and catalyst layer of both cathode and anode, and electrolyte membrane. Being all these components arranged one after the other, the total resistance of the cell will be the sum of the resistance of each component (Barbir, 2012; Liso & Araya, 2021):

$$R_{fc} = R_{gd,a} + R_{cl,a} + R_m + R_{cl,c} + R_{gd,c}$$

Eq. 38

Then, the ohmic losses due to the internal resistance of the fuel cell components is computed as:

$$\Delta V_{ohm} = R_{fc} I$$

Eq. 39

Where $R_{gd,a}$ and $R_{gd,c}$ are the resistance of the gas diffusion layers of anode and cathode respectively, $R_{cl,a}$ and $R_{cl,c}$ are the resistance of the two catalyst layers, R_m is the resistance of the membrane and I is the current flowing in the fuel cell. Moreover, the resistance of the membrane is strongly affected by the humidity of the fuel cell, so the ohmic losses are dependent on the humidity of the membrane.

2.4.3. Concentration (or mass transport) losses

The concentration losses are caused by the change of concentrations of the reactants at the surface of the electrodes and they become predominant for high level of current density. Furthermore, being the partial pressures of the reactants related with their concentrations, varying the concentrations also the partial pressures change. The resulting voltage drop due to the concentration losses is equal to:

$$\Delta V_{conc} = -\frac{RT}{nF}\ln\left(1 - \frac{i}{i_l}\right)$$

Eq. 40

Where i_l is the limit current density, i.e., the current value for which the fuel cell voltage is null. Concentration losses can be reduced increasing the conductivity of the electrodes, reducing the thickness of the electrodes, or improving the characteristics of the material of the bipolar plates.

2.4.4. Fuel crossover losses

Fuel crossover losses are present because part of the hydrogen and electrons can cross the electrolyte membrane. They are generally negligible with respect to the other losses and become relevant only at low temperatures.

2.4.5. Polarization curve

Considering all the losses mentioned before and subtracting them from the fuel cell OCV it is possible to obtain the relation between fuel cell voltage and current density.

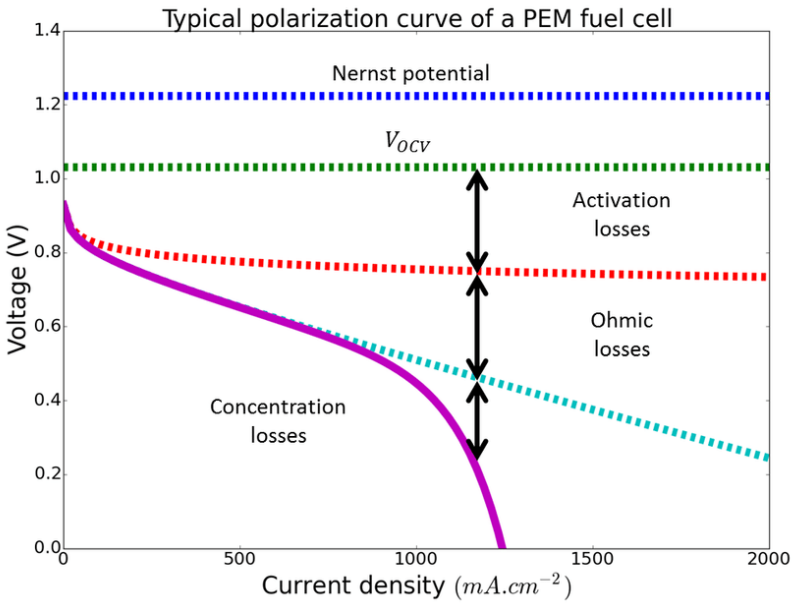

Fig. 2.3 (2 Typical Polarization Curve of a PEM Fuel Cell. | Download Scientific Diagram, n.d.)

The curve which represents this relation is called polarization curve, and it can be divided into three regions:

- A firsts non-linear region in which fuel cell voltage is subject to an abrupt voltage drop mainly due to the activation losses.
- A second region, in which the ohmic losses are predominant. Indeed, this region has an almost linear behaviour, and it is the operating region of the fuel cell.

- In the third region the concentration losses become important, and the curve is not linear anymore. The fuel cell voltage experiences a sharp voltage drop until the current density reaches the limit value and the fuel cell voltage is null.

The polarization curve represents the relation between the DC voltage at the cell terminals and the current density (current per unit membrane area) drawn by the external load. The energy conversion efficiency of a fuel cell can be computed as follows:

$$\eta_{conversion} = \frac{V(i)}{OCV}$$

Eq. 41

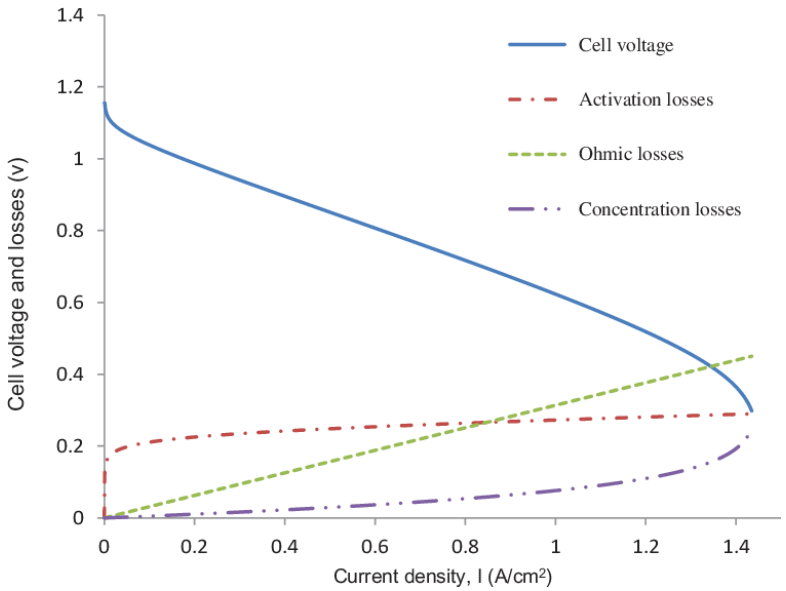

Fig. 2.4 (*Fuel Cell Voltage and Voltage Losses as a Function of Current Density... | Download Scientific Diagram*, n.d.)

2.5.Fuel cell operating conditions

Fuel cell operating conditions that must be considered are:

- Pressure
- Temperature
- Reactants flow rates
- Reactants humidity

These parameters are analysed below considering as case of study PEM fuel cell fed with pure hydrogen and air. Then, both fuel cell mass and energy balance are discussed.

2.5.1. Operating pressure

As seen in the Eq. 33 the fuel cell potential is proportional to the logarithm of pressure. Then it would be better to work with reactants at highest pressure as possible. Nevertheless, if the reactant is available at ambient pressure (as in the case of hydrogen/air PEM fuel cell), the power requested to pressurize the reactant may offset the gain obtained from fuel cell performance (Barbir, 2012; Bonci, 2021). Therefore, the best operating pressure depends on the entire fuel cell system. For the reactants which are stored in pressurized tank, as it is for the hydrogen, there is no power penalty for compression. Indeed, in hydrogen/oxygen fuel cells generally work at high pressure levels, usually between 3 and 12 bars and the pressure is controlled by a back pressure regulator which keeps the desired value of the pressure at the outlet. Instead, in case of the hydrogen/air fuel cells the air is supplied to the fuel cell through a blower or a compressor. Generally, fuel cell systems in which are used mechanical device for the air supply are used work at pressure up 3 bars. Also in this case the backpressure regulator may be present to pressurize the cell, otherwise it can be avoided and the gas is exhaust at ambient temperature (Barbir, 2012; Bonci, 2021).

Fig. 2.5 a) gas supply from high pressure tank, b) supply by a mechanical device, a compressor or blower (Barbir, 2012)

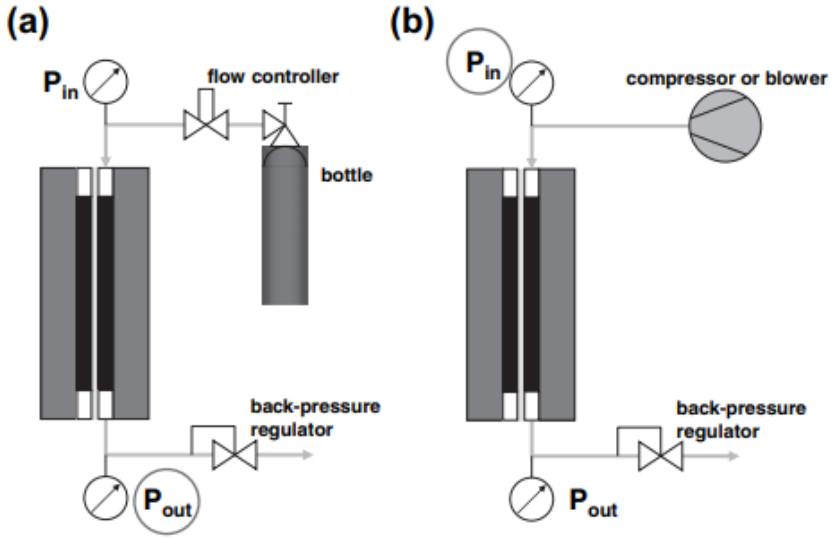

2.5.2. Operating temperature

Theoretically, at higher temperatures correspond higher fuel cell potentials. However, the optimal operating temperature depends on the fuel cell design. A PEM fuel cell can start working even at

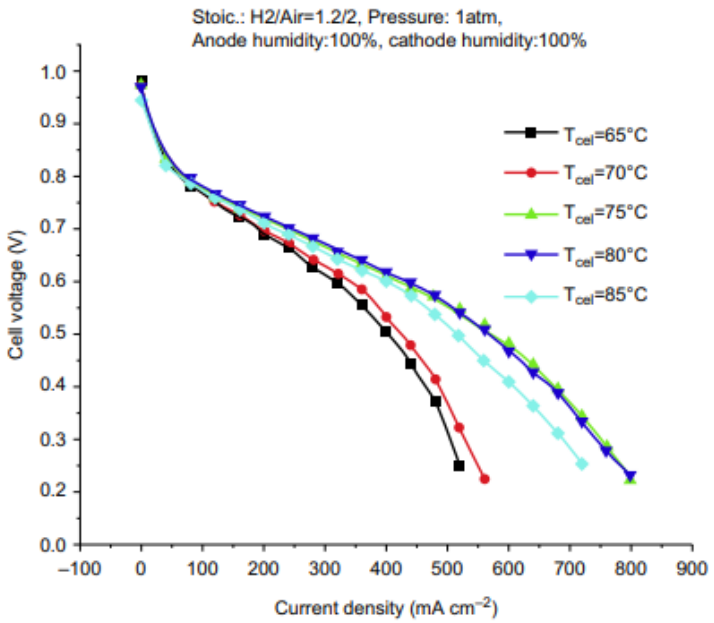

Fig. 2.6 Example of a PEM fuel cell polarization curve at different operating temperature (Barbir, 2012)

sub-zero temperatures (up to -30°C) without the need to be heated, even if this leads to a decrease in power (Barbir, 2012).

The upper limit temperature is 100 °C. The main functions of the membrane depend on its hydration and above 100°C the membrane can be dangerously dehydrated and can be damaged. This temperature is close to the glass transition temperature of the polymer. Then the PEM fuel cell are usually operated at temperature up to 80°C (Barbir, 2012; Bonci, 2021).

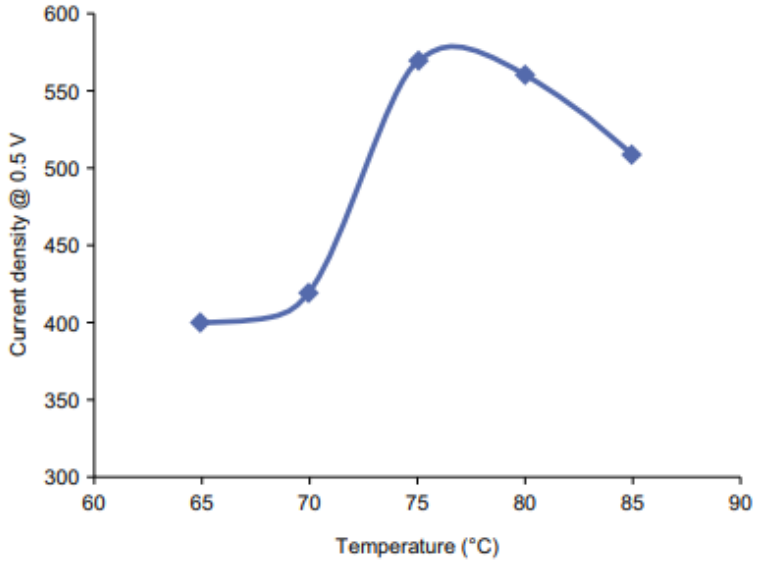

Fig. 2.7 Effect of temperature on fuel cell performance (Barbir, 2012)

Moreover, the operating temperature must be selected considering both the fuel cell performance and the system requirements, above all the size and power requirements for the heat management subsystem. To maintain the desired temperature, heat must be taken away from the fuel cell and often the heat dissipated from the outer surface of the fuel cell is not enough, so a cooling system is needed. The cooling medium may be air, water, or special coolant. The fuel cell heat balance is expressed as follows:

$$Q_{gen} + Q_{react_{in}} = Q_{react_{out}} + Q_{dis} + Q_{cool}$$

Eq. 42

Where Q_{gen} is the heat generated by the fuel cell, $Q_{react_{in}}$ and $Q_{react_{out}}$ are the heat brought into the cell by the reactant gases and that taken away by the living gases, Q_{dis} and Q_{cool} are the heat dissipated from the cell surface and the by the coolant respectively. Since the temperature inside a fuel cell may not be uniform, the cell temperature can be approximated by the following temperature (Barbir, 2012):

- Surface temperature
- Temperature of air leaving the cell
- Temperature of coolant leaving the cell

Generally, the air leaving the fuel cell or the coolant leaving the fuel cell are considered the better choices.

2.5.3. Reactant flow rates

The reactant flow rates have to meet the consumption of the reactants required by the fuel cell. Both the rate at which the reactants are consumed, and the water generation rate are computed using the Faraday's law:

$$\dot{N}_{H_2} = \frac{I}{2F};$$

Eq. 43

$$\dot{N}_{O_2} = \frac{I}{4F};$$

Eq. 44

$$\dot{N}_{H_2O} = \frac{I}{2F};$$

Eq. 45

Where $\dot{N}$ is the consumption rate of each reactant ($mols^{-1}$), I is the current (A), and F is the Faraday's constant ($Cmol^{-1}$). Multiplying for the molar mass of each species the mass flow rates of reactants' consumption and the mass flow rate of water generation are obtained (Barbir, 2012):

$$\dot{m}_{H_2} = \frac{I}{2F} M_{H2}$$

Eq. 46

$$\dot{m}_{O_2} = \frac{I}{4F} M_{O_2}$$

Eq. 47

$$\dot{m}_{H_2O} = \frac{I}{2F} M_{H_2O}$$

Eq. 48

The gases' flow rates may be expressed in volumetric units, that is, normal liters per minute ($Nlmin^{-1}$) or normal liters per second (Nls^{-1}), or normal cubic meters per hour (Nm^3h^{-1})(normal liter or normal cubic meter is a quantity of gas that would occupy 1 l or 1 m^3, respectively, of volume at atmospheric pressure, 101.3 kPa, and 0°C) . Often, in practice standard condition are used. However, since the standard conditions can vary from source to source, it is better to use normal liter or normal cubic meter which are SI unit. In normal conditions the molar volume of any gas is 22.414 $lmol^{-1}$. Following the order of magnitudes of the reactants consumption per Ampere and per cell are reported (Barbir, 2012; Bonci, 2021).

Table 3 Reactants' consumption rates (Barbir, 2012)

	Hydrogen consumption	Oxygen consumption	Water generation
$\frac{mol}{s}$	$5.18 * 10^{-6}$	$2.59 * 10^{-6}$	$5.18 * 10^{-6}$
$\frac{g}{s}$	$10.4 * 10^{-6}$	$82.9 * 10^{-6}$	$93.3 * 10^{-6}$
$Nlmin^{-1}$	$6.970 * 10^{-3}$	$3.485 * 10^{-3}$	-
Nm^3h^{-1}	$0.418 * 10^{-3}$	$0.209 * 10^{-3}$	-

The reactants may be supplied at the exact rate at which is being consumed, like the hydrogen, or in excess of consumption, as it is always necessary for the cathode side where water is produced and must be carried out from the cell with excess flow. The ratio between the actual reactant flow rate and the reactant consumption rate is the stoichiometric ratio:

$$S = \frac{\dot{N}_{act}}{\dot{N}_{cons}} = \frac{\dot{m}_{act}}{\dot{m}_{cons}} = \frac{\dot{V}_{act}}{\dot{V}_{cons}}$$

Eq. 49

While the fuel utilization is defined as the inverse of the stoichiometric ratio:

$$\eta_{fu} = \frac{1}{S}$$

Eq. 50

When the reactant is supplied with a stoichiometric ratio equal to unity (S=1), the supply mode is called dead-end mode. If the reactant, in this case pure hydrogen, is available at elevated pressure (for instance if it is stored in a high-pressure tank), dead-end mode doesn't require any controls. Even in dead-end mode it is important to purge the hydrogen because of accumulation of inert gases or water that can permeate the membrane. If the loss due to crossover permeation and that one due to purging are considered, the utilization is:

$$\eta_{fu} = \frac{\dot{N}_{H_{2_{cons}}}}{\dot{N}_{H_{2_{cons}}} + \dot{N}_{H_{2_{loss}}} + \dot{N}_{H_{2_{prg}}} \tau_{prg} f_{prg}}$$

Eq. 51

Where $\dot{N}_{H_{2prg}}$ is the rate of hydrogen purge, τ_{prg} is the duration of hydrogen purge and f_{prg} is the frequency of purge. Then, taking into account these losses the actual stoichiometric ratio of the hydrogen in dead-end supply mode is slightly higher than 1. The hydrogen purging can be avoided if it is supplied in excess, i.e., flow-through mode. In this case the fuel utilization is computed using the Eq. 50. Air is generally supplied in flow-through mode with a stoichiometric ratio $S \geq 2$ (but for S>3 the performance gain is very little). When pure reactants are used a recirculation mode can be used in order to recover the unused gases. Supplying air in flow-through mode has two advantages on fuel cell performance:

- Higher air flow rate helps to remove product water from the cathode.
- Higher air flow rate maintains oxygen concentration high.

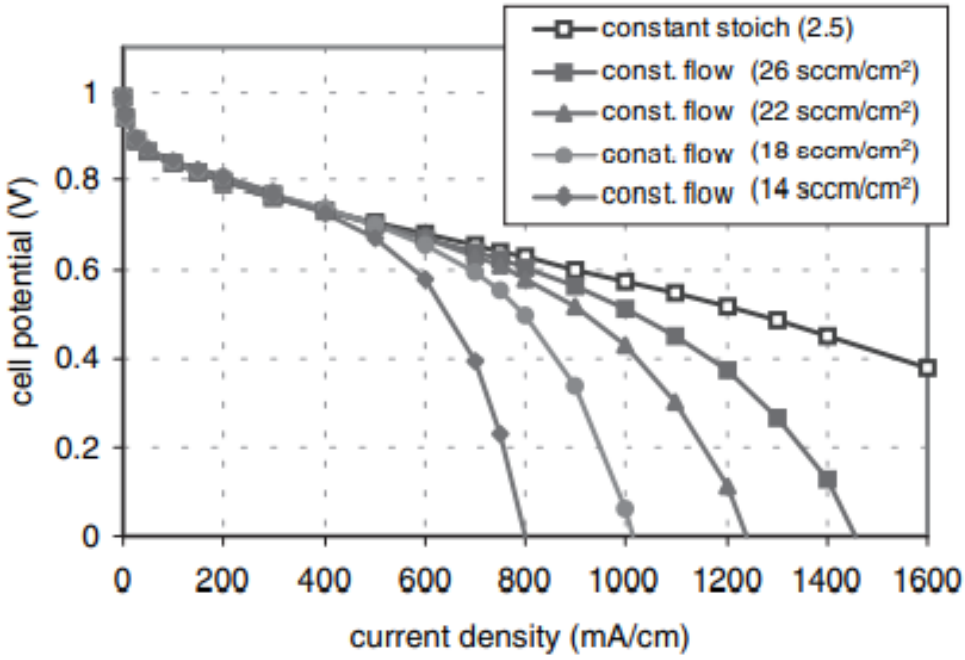

Fig. 2.8 Fuel cell performance at different air-flow rates (Barbir, 2012)

2.5.4. Reactants humidity

Due to the fact that polymeric membrane requires to maintain protonic conductivity, both reactant gases may be humidified before entering the cell. However, often excess humidity is needed on the anode side only, while the unsaturated conditions can be sufficient on the cathode side where water generation occurs (Barbir, 2012; Bonci, 2021). Following some parameters used to analyse the humidity conditions of the reactants are presented:

$$\text{The humidity ratio } x = \frac{m_v}{m_g}$$

Eq. 52

$$\text{The humidity molar ratio } \chi = \frac{N_v}{N_g} = \frac{p_v}{p_g} = \frac{p_v}{P - p_v}$$

Eq. 53

Which represent the ratio between the masses and the moles of water vapor and the dry gas, respectively. The humidity molar ratio can be also expressed as the ratio of the partial pressure of water vapor and the partial pressure of the dry gas. Obviously, multiplying the humidity molar ratio for the ratio between the molar mass of water and gas, the humidity ratio is obtained (Barbir, 2012).

$$\text{Relative humidity } \varphi = \frac{p_v}{p_{vs}}$$

Eq. 54

That is the ratio between the water vapor partial pressure and the maximum amount of water vapor that can be present in gas for given conditions (i.e., saturation pressure). Then, both the humidity ratio and the humidity molar ratio may be expressed in terms of relative humidity, saturation pressure, and total pressure by combining the previous equations (Barbir, 2012):

$$x = \frac{M_w}{M_a} \frac{\varphi p_{vs}}{P - \varphi p_{vs}}$$

Eq. 55

$$\chi = \frac{\varphi p_{vs}}{P - \varphi p_{vs}}$$

Eq. 56

Therefore, the vapor content by volume is (Barbir, 2012):

$$r_{H_2O_v} = \frac{\chi}{\chi + 1} = \frac{\varphi p_{vs}}{P}$$

Eq. 57

As shown in x the water vapor content in a gas diminishes increasing the total pressure and increases exponentially with temperature.

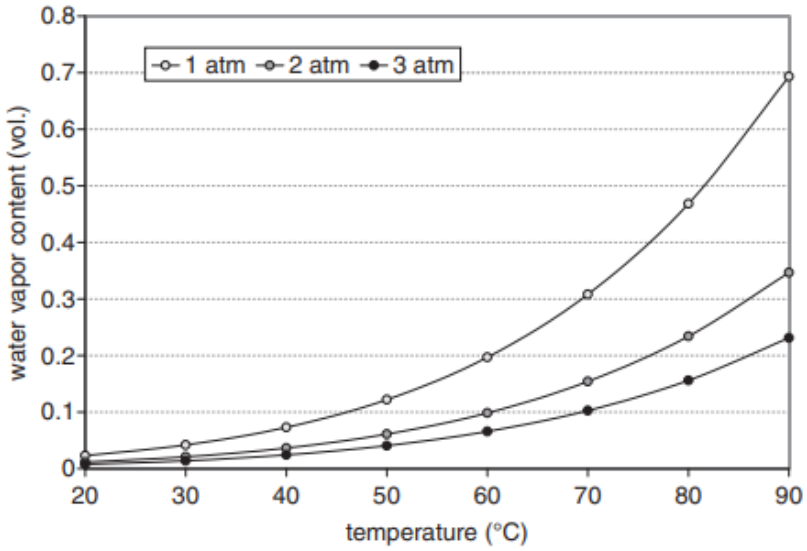

Fig. 2.9 Relation between water vapor content and temperature at different pressures (Barbir, 2012)

The reactants may be humidified through water or steam injection. Sometimes, both water and heat are required to get the operating condition from a dry gas or from ambient-temperature air. Injecting water in relatively dry gas would result in saturation at lower temperature than that of starting air and water.

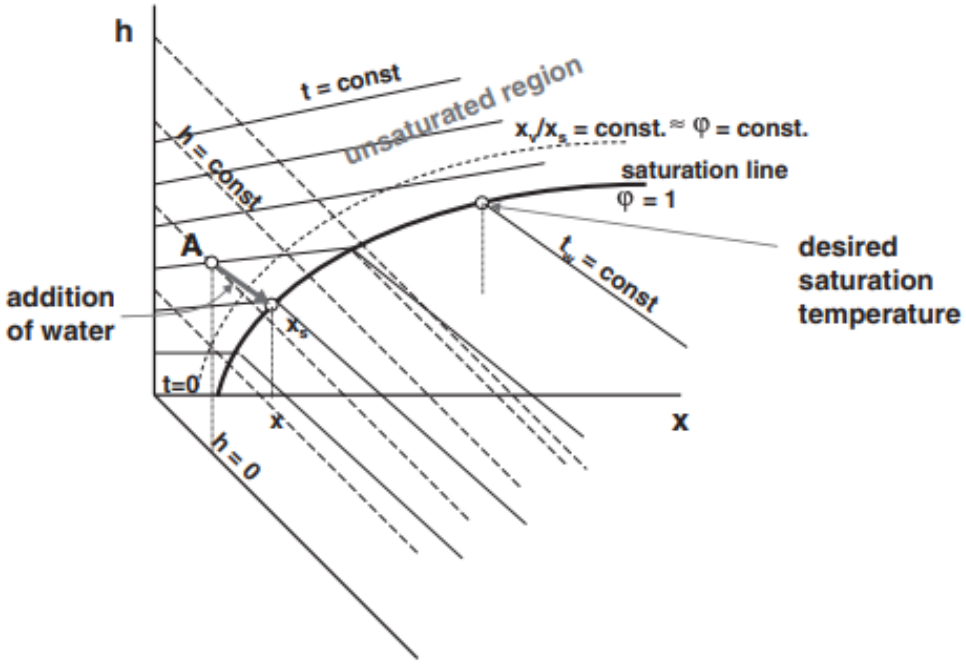

Fig. 2.10 Humidification process in a h-x diagram (Mollier diagram) (Barbir, 2012)

Usually, a fuel cell is able to produce enough heat and water to humidify the cathode electrode. Nevertheless, in real conditions, humidification is often still used to prevent the part of the membrane close to the air inlet from drying (Barbir, 2012; Bonci, 2021).

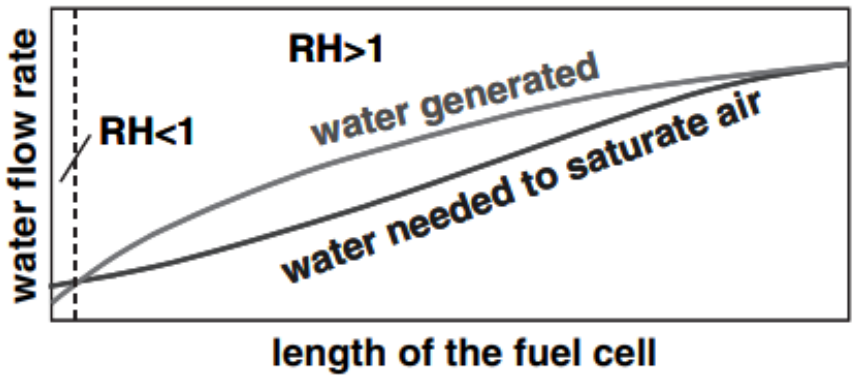

Fig. 2.11 Water profile in a fuel cell assuming realistic current density distribution and air temperature increase from inlet to outlet (Barbir, 2012; Bonci, 2021)

At low temperatures, small amounts of water are needed to saturate the air, so the water generated by the fuel cell is more than enough. Increasing the air temperature its pressure decreases and the amount of water needed increase. Then, with a careful design of air passages, heat transfer and water management, it is possible to closely match the water profile of the fuel cell.

Finally, in order to sum up, the typical operating conditions of a PEM fuel cell are listed in the following table.

Table 4 Typical PEM fuel cell operating conditions (Barbir, 2012)

	H_2/Air: ambient to 400kPa
Pressure	H_2/O_2: up to 1200 kPa
Temperature	50°C-80°C
Flow rates (S)	H_2: 1 to 1.2 O_2: 1.2 to 1.5 Air: 2 to 2.5
Humidity of reactants	H_2: 0 to 125% O_2/Air: 0 to 100%

2.5.5. Fuel cell mass balance

According to the fuel mass balance the sum of all mass input, that are fuel flow, oxidant flow and water vapor flow, must be equal to the sum of all mass outputs, namely the unused flows of fuel and oxidant plus water vapor present and liquid water present either fuel or oxidant exhaust (Barbir, 2012):

$$\sum(\dot{m}_i)_{in} = \sum(\dot{m}_i)_{out}$$

Eq. 58

Where i represent the species $H_2, O_2, N_2, H_2O_{(g)}$, and $H_2O_{(l)}$.

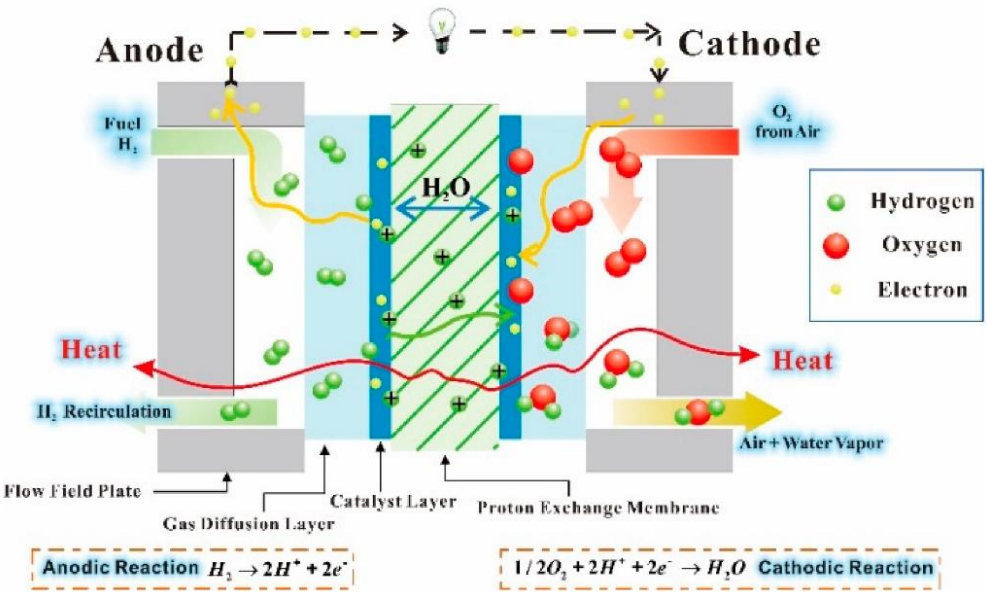

Fig. 2.12 PEM fuel cell schematization (Yuan et al., 2019)

Inlet flow rates

Since consumption of the reactants is proportional to the current and number of cells, all the inlet flow rates are proportional to current and number of cells too. In addition, considering that the cell power output is:

$$W_{el} = n_{cell} I V_{cell}$$

Eq. 59

Can be seen that all the flows are proportional to power output and inversely proportional to cell voltage:

$$n_{cell} I = \frac{W_{el}}{V_{cell}}$$

Eq. 60

Then, the mass flow of each species is computed below (Barbir, 2012).

Hydrogen mass flow rate (gs^{-1}) (we are considering pure hydrogen supply):

$$\dot{m}_{H_2 in} = S_{H_2} \dot{m}_{H_2 cons} = \frac{S_{H_2} M_{H_2}}{2F} In_{cell}$$

Eq. 61

Oxygen mass flow rate (gs^{-1}):

$$\dot{m}_{O_2 in} = \frac{S_{O_2} M_{O_2}}{4F} In_{cell}$$

Eq. 62

Air mass flow rate (gs^{-1}):

$$\dot{m}_{Air_{in}} = \frac{S_{O_2}}{r_{O_2}} \frac{M_{Air}}{4F} In_{cell}$$

Eq. 63

Nitrogen (which occupies 79% of air by volume at the fuel cell inlet) flow rate (gs^{-1}):

$$\dot{m}_{N_2 in} = \frac{S_{O_2} M_{N_2}}{4F} \frac{1 - r_{O_{2in}}}{r_{O_{2in}}} In_{cell}$$

Eq. 64

Water vapor present in hydrogen inlet (gs^{-1}):

$$\dot{m}_{H_2 O in H_2 in} = \frac{S_{H_2} M_{H_2 O}}{2F} \frac{\varphi_{an} P_{vs(T_{am,in})}}{P_{an} - \varphi_{an} P_{vs(T_{am,in})}} In_{cell}$$

Eq. 65

Where φ_{an} is the relative humidity at hydrogen inlet at the anode.

Water vapor present in the air inlet (gs^{-1}):

$$\dot{m}_{H_2 O in Air in} = \frac{S_{O_2} M_{H_2 O}}{r_{O_2} 4F} \frac{\varphi_{cat} P_{vs(T_{am,in})}}{P_{cat} - \varphi_{cat} P_{vs(T_{am,in})}} In_{cell}$$

Eq. 66

Outlet flow rates

The unused hydrogen flow rate is:

$$\dot{m}_{H_2 out} = \frac{(S_{H_2} - 1) M_{H_2}}{2F} In_{cell}$$

Eq. 67

The water content of hydrogen at the exhaust is the difference between water brought into the cell with the gas and net water transport across the membrane, which is due to the electroosmotic drag (from anode to cathode) and water back diffusion (from cathode to anode)(Barbir, 2012).

Water balance in the cathode:

$$\dot{m}_{H_2 O in H_2 out} = \dot{m}_{H_2 O in H_2 in} - \dot{m}_{H_2 OED} + \dot{m}_{H_2 OBD}$$

Eq. 68

Where $\dot{m}_{H_2 OED}$ is the amount of water transport due to the electroosmotic drag which is equal to:

$$\dot{m}_{H_2 OED} = \frac{\zeta_D M_{H_2 O}}{E} In_{cell}$$

Eq. 69

$$\dot{m}_{H_2OBD} = \beta \frac{\zeta_D M_{H_2O}}{E} In_{cell}$$

Eq. 70

$\zeta_D$is the electroosmotic drag coefficient, which represents the number of water molecules per proton. Water concentration inside the fuel cell is not uniform and is not easy to explicitly compute the back diffusion for the entire cell. So, back diffusion is expressed as a fraction, β, of the electroosmotic drag (Barbir, 2012).

The maximum amount of vapor at the exhaust (saturation condition):

$$\dot{m}_{H_2OinH_2out,V} = \min\left[\frac{(S_{H_2} - 1)M_{H_2O}}{2F} \frac{P_{vs(T_{out,an})}}{P_{an} - \Delta P_{an} - P_{vs(T_{out,an})}} In_{cell}, m_{H_2OinH_2out}\right]$$

Eq. 71

Where ΔP_{an} is the pressure drop on the anode side.

The amount of liquid water, if any, is:

$$\dot{m}_{H_2OinH_2out,L} = \dot{m}_{H_2OinH_2out} - \dot{m}_{H_2OinH_2out,V}$$

Eq. 72

Oxygen flow rate at the exhaust:

$$\dot{m}_{O_2out} = \frac{(S_{O_2} - 1)M_{O_2}}{4F} In_{cell}$$

Eq. 73

Nitrogen flow rate at the outlet is the same of the flow rate at the inlet because it does not participate in the fuel cell reaction:

$$\dot{m}_{N_2out} = \dot{m}_{N_2in} = \frac{S_{O_2} M_{N_2}}{4F} \frac{1 - r_{O_{2in}}}{r_{O_{2in}}} In_{cell}$$

Eq. 74

The air flow rate at the outlet is the sum of oxygen and nitrogen flow rates:

$$\dot{m}_{Airout} = \frac{\left[(S_{O_2} - 1)M_{O_2} + \frac{S_{O_2}(1 - r_{O_{2in}})}{r_{O_{2in}}} M_{N_2}\right] In_{cell}}{4F}$$

Eq. 75

The amount of water at the cathode exit is the sum of the water brought in the cell by humid air at the inlet, the water generated, and the net water transport across the membrane (Barbir, 2012).

$$\dot{m}_{H_2OinAirout} = \dot{m}_{H_2OinAirin} + \dot{m}_{H_2Ogen} + \dot{m}_{H_2OED} - \dot{m}_{H_2OBD}$$

Eq. 76

The maximum possible water vapor flux at the cathode outlet is:

$$\dot{m}_{H_2OinAirout,V} = \min\left[\frac{(S_{O_2} - r_{O_{2in}})M_{H_2O}}{r_{O_{2in}}\,4F}\frac{P_{vs(T_{out,an})}}{P_{cat} - \Delta P_{cat} - P_{vs(T_{out,an})}}In_{cell}, m_{H_2OinAirout}\right]$$

Eq. 77

And ΔP_{cat} is the pressure drop on the cathode.

The amount of liquid water, if there is, is equal to:

$$\dot{m}_{H_2OinAirout,L} = \dot{m}_{H_2OinAirout} - \dot{m}_{H_2OinAirout,V}$$

Eq. 78

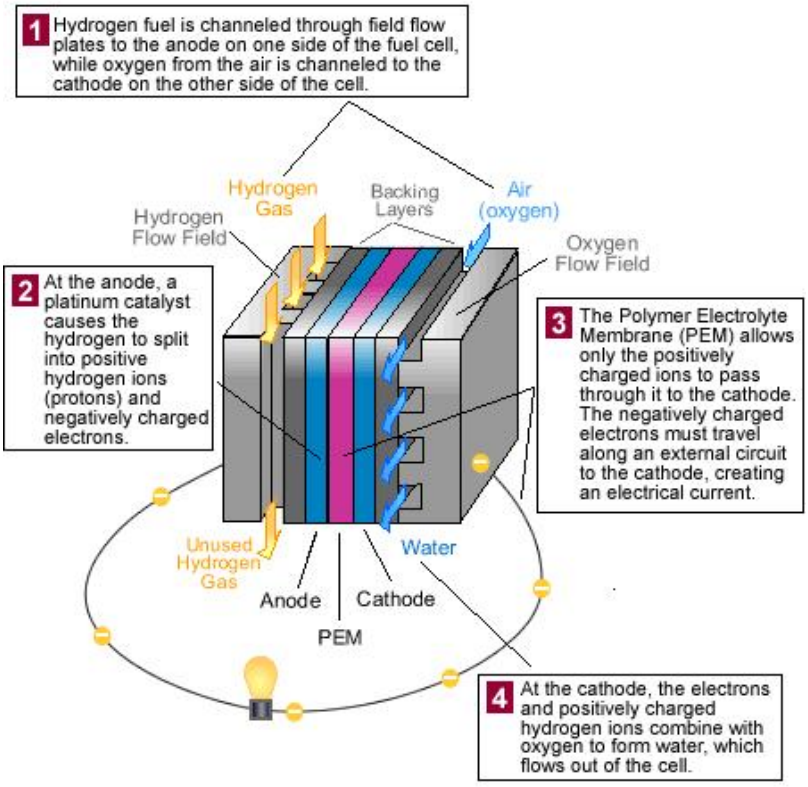

Fig. 2.13 PEM fuel cell (*How Fuel Cells Work*, 2023)

2.5.6. Fuel cell energy balance

Applying the energy balance at the fuel cell, the energy inputs are the enthalpies of all the flows into the fuel cell, that are hydrogen and air, and the enthalpy of water present in those gases. While, the energy outputs are the electric power produced, the enthalpies of the flows out of the fuel cell (so, unused fuel and oxidant and water present in both fuel and oxidant), and heat flux out of the fuel cell (which include both the heat dissipated by cooling and the heat dissipated from the fuel cell surface(Barbir, 2012):

$$\sum(H_i)_{in} = W_{el} + \sum(H_i)_{out} + Q$$

Eq. 79

The enthalpy (Js^{-1}) for each dry gas, or a mixture of dry gases, is calculated as:

$$H = \dot{m} c_p t$$

Eq. 80

If a gas is combustible, its enthalpy is:

$$H = \dot{m}(c_p t + h^0_{HHV})$$

Eq. 81

Where h^0_{HHV} is the higher heating value (Jg^{-1}) of that gas at 0°C. Usually, the heating values are reported in table at 25°C. The difference between h^{25}_{HHV} and h^0_{HHV} is the difference of the enthalpies of reactants and products at those temperatures. So, h^0_{HHV} for the hydrogen is:

$$h^0_{HHV} = h^{25}_{HHV} - \left(c_{p,H_2} + \frac{1}{2}\frac{M_{O_2}}{M_{H_2}} c_{p,O_2} - \frac{M_{H_2O}}{M_{H_2}} c_{p,H_2O(l)} \right) 25$$

Eq. 82

The enthalpy of water vapor is:

$$H_{H_2O,v} = \dot{m_{H_2O(g)}}(c_{p,H_2O(g)} t + h^0_{fg})$$

Eq. 83

Where h^0_{fg} is the heat of evaporation of the water at 0°C. Instead, the enthalpy of liquid water is:

$$H_{H_2O,l} = \dot{m_{H_2O(l)}} c_{p,H_2O(l)} t$$

Eq. 84

3. Fuel cell system and auxiliaries

As it was shown in the previous chapter, a fuel cell can reach a very low voltage ($V_{cell} < 1V$) in actual conditions. Then, to match the power needed by the load several fuel cells must be connected in series, assembling the so-called fuel cell stack. In this way, the active area and the thickness of the cables can be reduced maintaining low resistive losses.

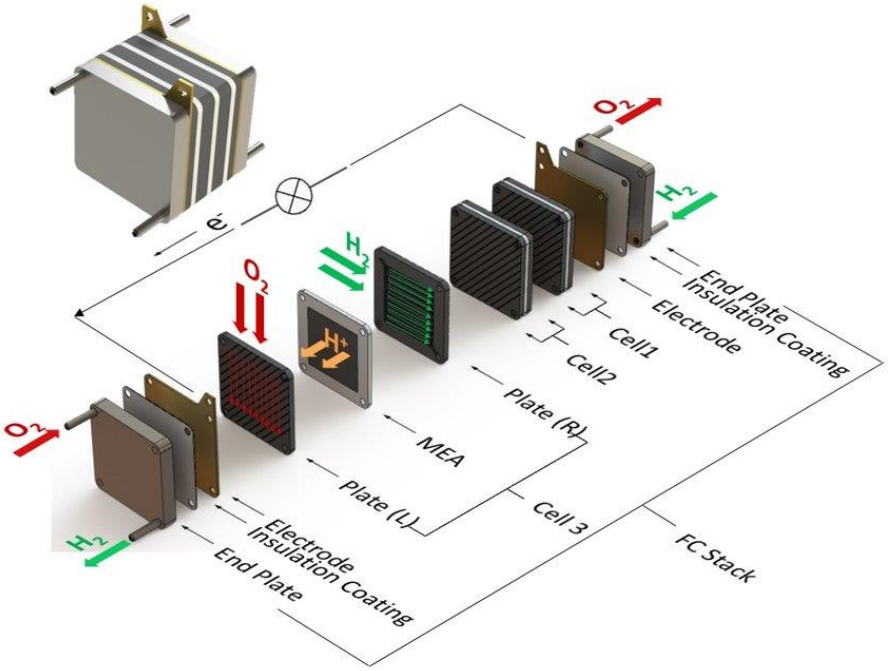

Fig. 3.1 Fuel cell stack example(Sutharssan et al., 2016)

The stack potential is computed summing up the individual cell voltages, V_{cell}, which are dependent on current density i according to their polarization curves. However, having several cells (in automotive field a single stack may be composed of 200-300 cells) the stack potential can be calculated more easily as the product of average individual cell potential and number of cells in the stack:

$$V_{stk} = \sum_{i=1}^{n_{cell}} V_i = \overline{V_{cell}} n_{cell}$$

Eq. 85

Then, the stack power output is equal to the product of the stack voltage and the current $I = iA_{cell}$ (where A_{cell} =fuel cell active area):

$$P_{stk} = V_{stk} I$$

Eq. 86

The fuel cell stack efficiency can be computed as:

$$\eta_{stk} = \frac{P_{stk}}{\dot{m}_{H_2} HHV}$$

Eq. 87

However, the fuel cell stack needs several auxiliary subsystems to work properly. The subsystem which are typically involved for a hydrogen/air fuel cell system are:

- Oxidant supply
- Hydrogen supply
- Heat management
- Water management
- Power conditioning
- Instrumentation and control

All these subsystems require part of the power generated by the fuel cell stack, P_{aux}. Therefore, the system efficiency is obtained through the formula (Barbir, 2012; Bonci, 2021):

$$\eta_{stk,sys} = \frac{P_{stk} - P_{aux}}{\dot{m}_{H_2} HHV}$$

Eq. 88

Otherwise, taking into account that the efficiency of propulsion systems based on ICE is computed considering the lower heating value, LHV, in order to compare the efficiencies of the two types of propulsion system both the fuel cell stack efficiency and the system efficiency may be computed as:

$$\eta_{stk} = \frac{P_{stk}}{\dot{m}_{H_2} LHV}$$

Eq. 89

$$\eta_{stk,sys} = \frac{P_{stk} - P_{aux}}{\dot{m}_{H_2} LHV}$$

Eq. 90

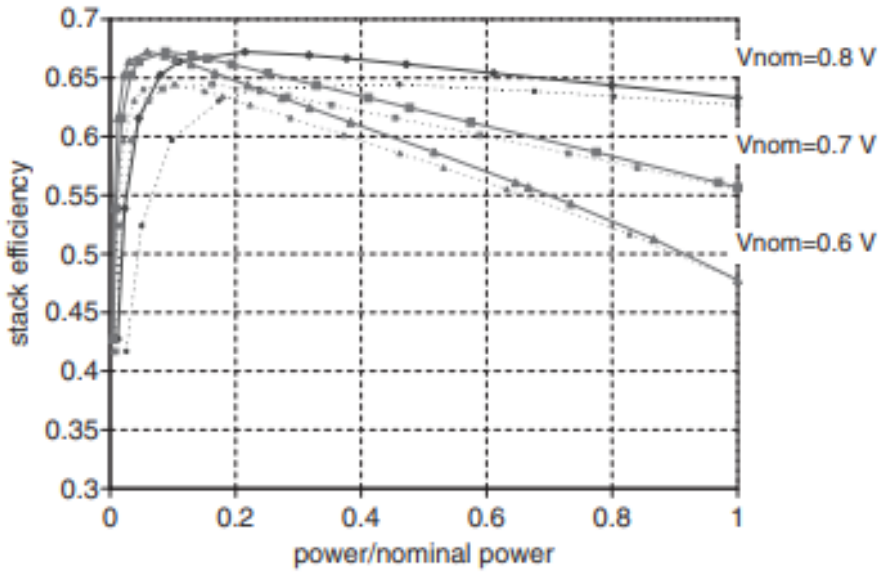

Fig. 3.2 FC stack effiency based on LHV vs FC power output for different nominal cell potential (Barbir, 2012).

3.1.Air supply system

In hydrogen/air systems, according to both the dimensions and power of the fuel cell there are different way to supply air from the external environment (Barbir, 2012; Bonci, 2021):

- For very small power outputs passive air supply (relying only on natural convection)
- For low pressure system air may be supplied by a fan or a blower
- For pressurized system the air is supplied by a compressor, in this case a pressure regulator is needed at the fuel cell outlet.

Anyway, to use a mechanical device to supply air into the fuel cell requires some power from the fuel cells which represent a power loss for the system. Considering the compression as an adiabatic compression, the ideal power needed for the adiabatic compression of air from P_1 to pressure P_2 is:

$$P_{comp_{id}} = \dot{m}_{Air_{in}} c_p T_1 \left[\left(\frac{P_2}{P_1} \right)^{\frac{k-1}{k}} - 1 \right]$$

Eq. 91

Where $\dot{m}_{Air_{in}}$ is the air flow rate (gs^{-1}), c_p is the specific heat ($Jg^{-1}K^{-1}$), T_1 is the temperature before compression (K), P_1 and P_2 are respectively the pressure before and after the compression, and k is the ratio of specific heats (for diatomic gases is equal to 1.4).

Nevertheless, considering the inefficiencies related with the compression the power needed to increase the pressure is higher than the ideal adiabatic power:

$$P_{comp} = \frac{\dot{m}_{Air_{in}}}{\eta_{comp}} c_p T_1 \left[\left(\frac{P_2}{P_1} \right)^{\frac{k-1}{k}} - 1 \right]$$

Eq. 92

Where η_{comp} is the efficiency of the compression and is equal to the ratio between the ideal (adiabatic) and the actual compression power. The temperature at the end of compression can be obtained from the energy balance:

$$T_2 = T_1 + \frac{T_1}{\eta_{comp}} \left[\left(\frac{P_2}{P_1} \right)^{\frac{k-1}{k}} - 1 \right]$$

Eq. 93

Obviously, the electric power needed by the electric motor to pressurize the air is even larger. Then, considering the mechanical and electrical efficiencies, the electric power needed by the device is(Barbir, 2012):

$$P_{em} = \frac{P_{comp}}{\eta_{mech} \eta_{em}}$$

Eq. 94

Generally, two types of compressors are used in pressurized fuel cell systems:

- Positive displacement compressors, in which the flow rate may be changed without the need to change back pressure by simply reducing the speed of the motor.
- Centrifugal compressors (radial or axial), which have different pressure-flow rate characteristics. They must not be operated at low-flow region left of the surge line. So, the flow regulation and pressure regulation must be done together, obtaining high efficiencies through a wide range of flow rates (Barbir, 2012; Bonci, 2021).

In pressurized systems, the air at the fuel cell outlet is warm and still pressurized. The energy contained in the gas may be exploited in an expander or a turbine to generate work and may offset the work needed to air compression. The compressor and the turbine may be installed on the same shaft, obtaining a turbo-compressor.

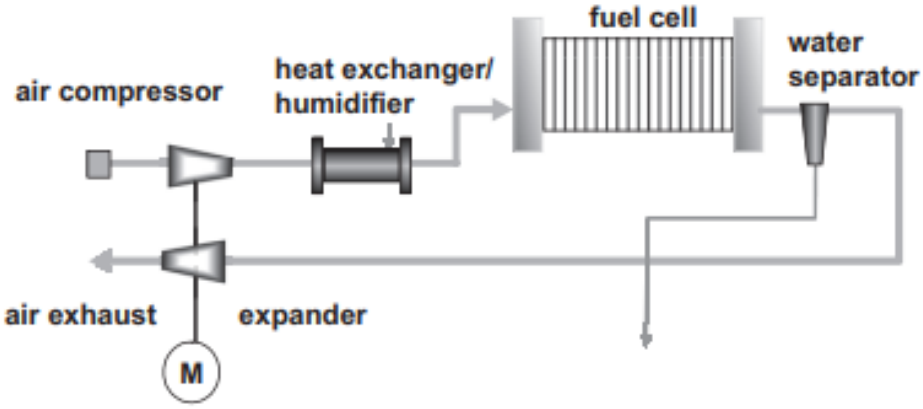

Fig. 3.3 Schematic diagram of a fuel cell system with an expander at the exhaust (Barbir, 2012)

The available power that can be extracted from the outlet air, expanding it from outlet pressure, P_{out}, to the ambient pressure is:

$$P_{exp} = \dot{m}_{Air_{out}} c_p T_{out} \left[1 - \left(\frac{P_{amb}}{P_{out}} \right)^{\frac{k-1}{k}} \right] \eta_{exp}$$

Eq. 95

Where η_{exp} is the ratio between the actual expansion work and the ideal isentropic work between the two pressures.

The temperature at the end of the expansion is:

$$T_{end} = T_{out} - T_{out} \left[1 - \left(\frac{P_{amb}}{P_{out}} \right)^{\frac{k-1}{k}} \right] \eta_{exp}$$

Eq. 96

However, due to the inefficiencies and the pressure drop through the stack, the power recovered is only part of the compression work(Barbir, 2012).

3.2. Hydrogen supply system

Despite requiring a lot of space, the systems with hydrogen storage are much simpler and more efficient. Usually, hydrogen is stored in high-pressure cylinders. Typical storage pressures are between 200 bars and 450 bars and even 690 bars, instead, in the automotive field the two most used pressures are 350 bars and 700 bars. After hydrogen is released from the high-pressure tank, there are two ways to supply hydrogen to a fuel cell (Barbir, 2012; Bonci, 2021):

- The dead-end mode, that is the simplest method. These systems require only a pre-set pressure regulator. However, in dead-end mode work in long-term operation extremely pure reactant gases are needed. The impurities and inert gases may be accumulated in both anode and cathode. To avoid this issue, hydrogen can be purged periodically.
- The flow-through mode, it is used when purging hydrogen is not possible. The hydrogen is supplied in excess (S>1) and the unused hydrogen is returned to the inlet using either passive device, like an ejector, or active device, like a compressor or a pump. It would be preferred that water is separated and collected.

Sometimes, in hydrogen/air systems the hydrogen present in the fuel cell exhaust is used in a burner to generate more heat, which then may be used to provide additional work through a turbine or an expander.

Furthermore, hydrogen usually is humidified up to saturation condition before entering the fuel cell stack to avoid drying the membrane. Hydrogen may be humidified by water injection and simultaneously or subsequently heated to facilitate water evaporation, or by membrane humidification, which allows both water and heat exchange (Barbir, 2012).

3.3. Water management and humidification schemes

As previous mentioned, water plays a key role in fuel cell performance. It is important to humidify hydrogen to ensure that the electroosmotic drag does not dry out the membrane on the anode side. Air must be humidified to avoid that the excess of dry gas removes water at a rate higher than water generation rate of the fuel cells (Barbir, 2012).

Air humidification may be achieved by:

- Bubbling the gas through water
- Direct water or steam injection
- Exchange of water and heat through a water-permeable medium
- Exchange of water and heat on an absorbent surface

The first one is often used in laboratory but rarely in practical systems. Direct water injection is a more compact method and is easier to manage. The required quantity of water to be injected is computed through the following formula:

$$\dot{m}_{H_2O} = \frac{\dot{m}_{Air} M_{H_2O}}{M_{Air}} \left(\frac{\varphi P_{sat}(T)}{P - \varphi P_{sat}(T)} - \frac{\varphi_{amb} P_{sat}(T_{amb})}{P_{amb} - \varphi_{amb} P_{sat}(T)} \right)$$

Eq. 97

Where $\varphi, T, P,$ and $\varphi_{amb}, T_{amb},$ and P_{amb} are respectively relative humidity, temperature, and pressure at the fuel cell inlet and of the ambient air. The water must be injected in the form of mist to have the contact area between water and air as large as possible making the evaporation easier. The humidification process need heat for the evaporation. The fuel cell stack itself produce enough heat humidify the reactants. Direct steam injection does not require additional heat exchange, nevertheless, the steam must be produced somewhere. Then, it is not usable for low temperature PEM fuel cells(Barbir, 2012).

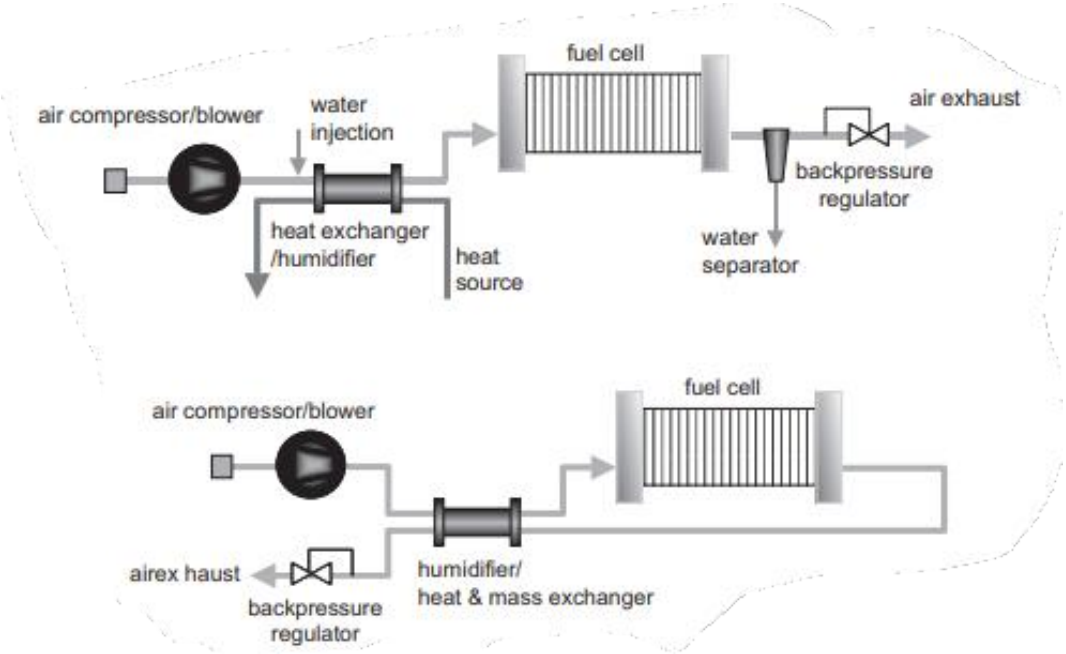

Fig. 3.4 Water injection scheme with heat exchange (above); exchange of water and heat with cathode exhaust (below) (Barbir, 2012)

The exchange of heat and water from the cathode exhaust with incoming air take advantage of water and heat produced by the fuel cell stack. A water-permeable medium, like a porous plate (metal, ceramic, or graphite) or water-permeable membrane (Nafion) or through an enthalpy wheel (when an absorbent surface is used). These devices are mass and heat exchangers, enabling the water and heat exchange between warm and oversaturated fuel cell exhaust and dry incoming air. At operating conditions these methods cannot humidify the reactant up to 100% of relative humidity. In this case the membrane can be humidified intermittently short-circuiting the fuel cell stack for short period of time, creating more water in the cathode side (Barbir, 2012).

Water and heat management may be integrated together if deionized water is used as stack coolant. However, if the fuel cell stack may operate at sub-zero temperatures the presence of water in the system makes it susceptible to freezing. Then, the coolant loop must be separated from the water system and antifreeze coolants is used instead deionized water (Barbir, 2012; Bonci, 2021). One way to keep the system warm is to operate (periodically or constantly) the fuel cell at low power levels, decreasing the efficiency and so increasing the heat released by the stack. Another option is to drain the water from the system at shut down.

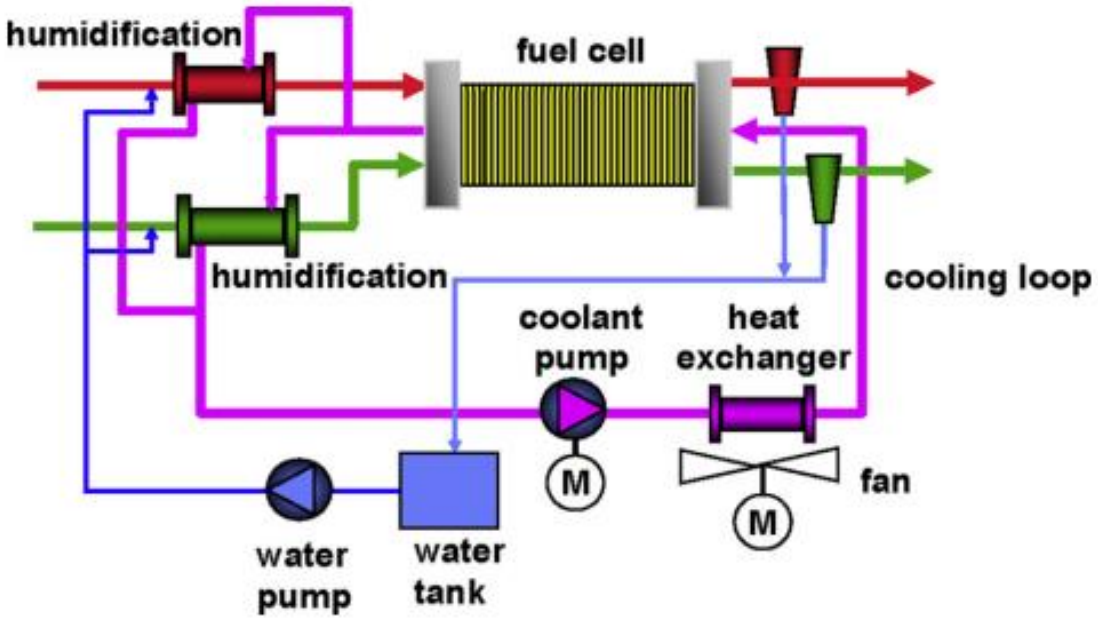

Fig. 3.5 Fuel cell system with separate subsystems: water for humidification and antifreeze coolant for cooling (Barbir, 2012)

3.4.Thermal management systems and waste heat recovery (WHR) method

Effective management of the heat produced by the fuel cell stack, by cooling, is very important to maintain the cells at a uniform operating temperature avoiding that an excessive operative temperature may dry out the membrane and reduce the surface area of the catalyst and enhancing the durability and the fuel cell performance. Furthermore, exploiting the heat removed from the fuel cell by cooling through the use of waste heat recovery technologies can add a great economic value to the PEMFC power system. The cooling strategy for the thermal management of the fuel cell depends on the power and application of the stack. The cooling systems may be grouped into two families:

- Passive cooling, in which the heat is removed by natural convection, conduction and radiation modes without any external device.
- Active cooling, where the heat transfer is improved by the action of an external device, such as a blower or a compressor. In some cases, the thermal management via active cooling may need a controller, such as a proportional integral controller (PI), to regulate the main operation parameters of the system.

The heat power extracted from the system may be converted back to electricity, mechanical power, or may be used as thermal energy in specific functions recovering some energy and improving the system efficiency.

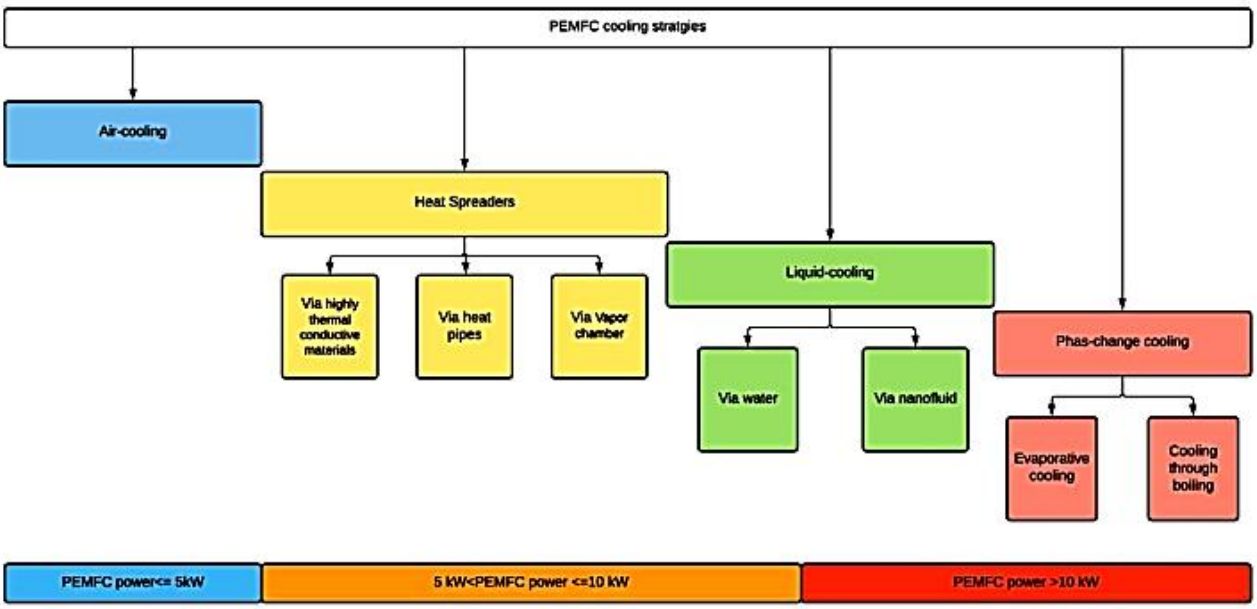

Fig. 3.6 PEMFC cooling strategies (Baroutaji et al., 2021a)

.

3.4.1. Thermal management strategies of PEMFC stacks

As mentioned before, thermal management of the PEMFC consist of extract the heat produced by the device keeping its temperature at the designed operational value. The most suitable cooling method depends mainly on the power level of the device (Baroutaji et al., 2021b).

Passive cooling techniques

In passive cooling the cooling is ensured by heat spreaders, heat pipes, or vapor chambers. Since in passive cooling the heat is dissipated without any external device, it has several advantages: it is simple, it has a high energy efficiency and low noise, due to the absence of external devices, it is easy to implement and cheap. Nevertheless, the absence of an external device leads to a low cooling capacity, so it can be used only for small PEMFC.

Active cooling techniques

In the active cooling the heat is absorbed by a cooling fluid which passes through the stack increasing its temperature. Therefore, the heat extracted by the fluid may be directly released to the environment using a radiator or it may be used for other purposes, and then dissipated to the surrounding environment. There are three types of active cooling, which differ for the cooling fluid utilized: air-cooling, liquid-cooling, in which the cooling medium may be water or other type of liquids, and the phase-change cooling.

Air-cooling

In this cooling strategy, the cooling fluid is air, and it can pass either in the cathode or in dedicated cooling plates. The channels design plays a significant role in the cooling effectiveness of the system. Despite its simplicity and its good characteristics (above all if integrated with cooling channels passing into the cathode), air-cooling is suitable for small PEMFCs with low power.

Indeed, in larger power applications this system is not able to face the increase of parasitic losses (Barbir, 2012; Baroutaji et al., 2021b).

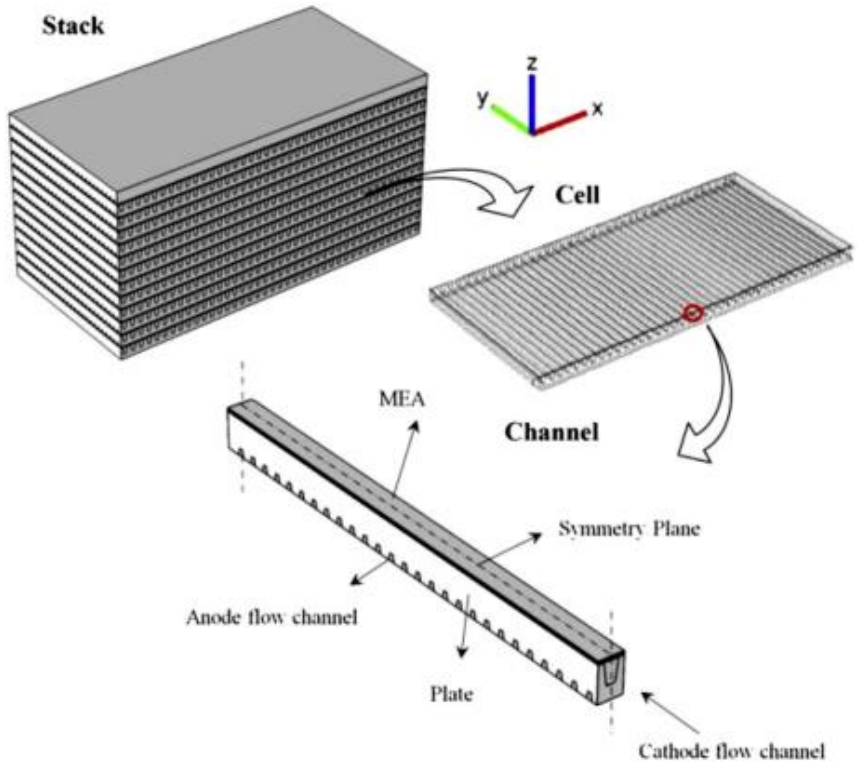

Fig. 3.7 PEMFC with combined oxidant and cooling channels(Baroutaji et al., 2021b)

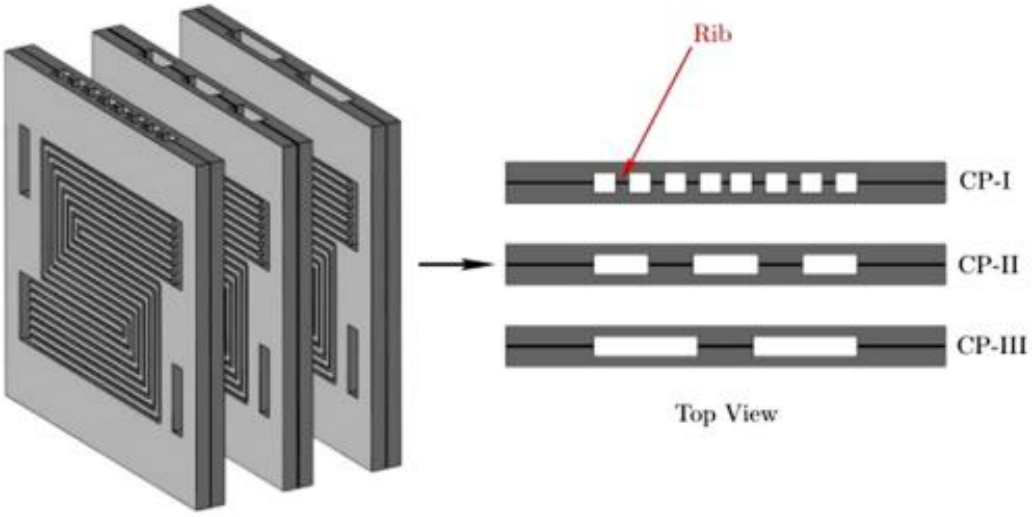

Fig. 3.8 Cooling plates designs examples (Baroutaji et al., 2021b)

Liquid-cooling

Liquid cooling systems use water or other liquid fluids, such as glycol-water mixture or nanofluids, depending on the type of application, especially on the temperature range and the thermal power that has to be managed. If compared to the air-cooling system, thanks to the greater specific heat of the water, the liquid-cooling has a better cooling effectiveness and smaller heat exchanger for the same amount of it to be removed. Indeed, it is a better choice for high cooling loads and for large PEMFC with power greater than 5 kW, for instance, for the in fuel cell electric vehicle (FCEV) (Barbir, 2012; Baroutaji et al., 2021b). The most used working fluid is the deionized water. Using deionized water enables the integration of water and heat management of the fuel cell . In a conventional liquid cooling system, the water flows into the cooling channels in the bipolar plates (or in dedicated cooling plates) absorbing the fuel cell heat, then goes to the radiator where the heat is dissipated by the fan into the environment, and once the water temperature is decreased it is send to the PEMFC by the pump to repeat the loop.

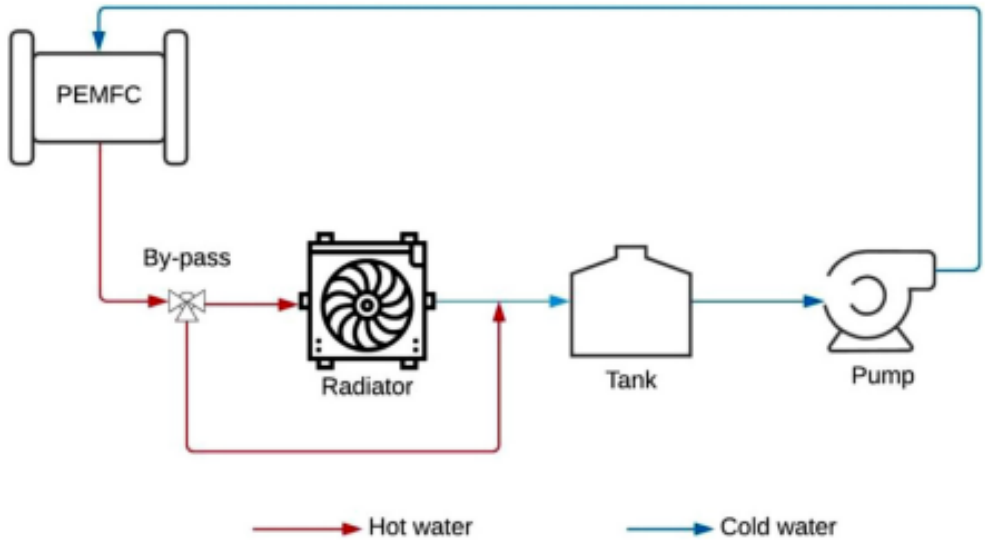

Fig. 3.9 Typical liquid-cooling cycle (Baroutaji et al., 2021b)

Like in the air-cooling case, the cooling performance of the system is strongly affected by geometry of the flow channels. According to different studies in which different channel schemes and geometry have been compared, it turned out that the zig-ag configuration of the channels shape and the multi-pass serpentine (MPSFF) are the best designs between among those tested in numerical simulations (Baroutaji et al., 2021b).

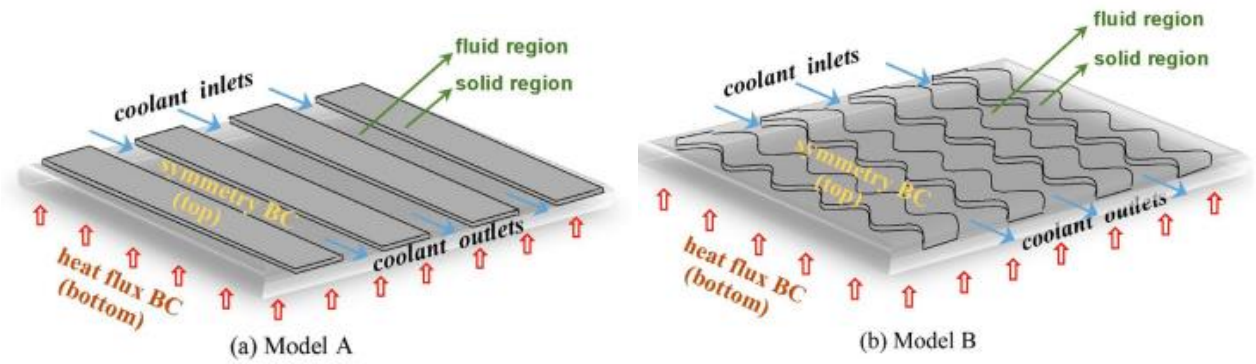

Fig. 3.10 Straight flow channels (model A) and zig-zag flow channels (model B) (Baroutaji et al., 2021b)

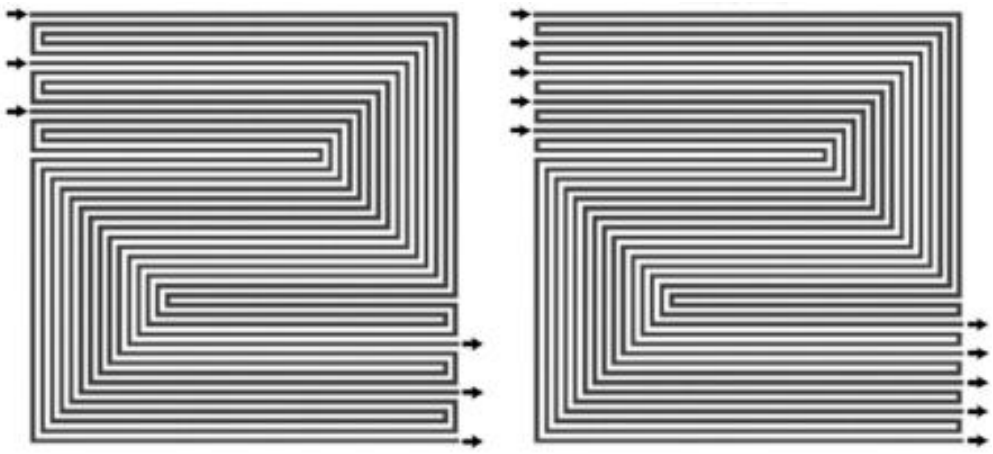

Fig. 3.11 MPSFF coolant flow fields (Baroutaji et al., 2021b)

Another interesting option is to use nanofluids as cooling fluid. They are obtained dispersing nanoscale metallic and non-metallic particles into a liquid cooling medium, such as water, obtaining the following improvements:

- Firstly, the suspended nanoparticles are characterized by a large specific surface which improves considerably the thermal characteristics of the nanofluids (thermal conductivity, convective heat transfer coefficient, thermal diffusivity and viscosity).
- The nanoparticles can immobilize the ions from the base fluid avoiding the usage of deionizing filter within the cooling cycle.
- Some nanofluids are able to operate at sub-zero temperatures thanks to their lower freezing point, which is important for those applications in extremely cold weather.
- Eventually, nanofluids, having better heat transfer properties, enable the reduction of the heat exchanger size and the parasitic losses of the system.

The only drawback reported is that both the pressure drop and the voltage drop are increased when nanoparticles are used.

Phase change cooling

This cooling method employ the latent heat of a phase change material (PCM) to absorb the heat of a PEMFC stack. Comparing it with the liquid-cooling system it has been observed that the phase change cooling allow to reduce both the cooling flow rate and the parasitic losses, decreasing the pumping requirements, and to maintain a more uniform temperature distribution. Phase change cooling can be either evaporative cooling or two-phase cooling with boiling.

The evaporative cooling is achieved through the injection of liquid water in the air-flow channels with both fuel and oxidant. Flowing through the fuel cells the injected water evaporates absorbing the heat produced by the fuel cell stack and humidifying the membrane enhancing its protonic conductivity. Once the water vapor has been exhausted, it passes through a condenser to be converted again into liquid water and stored in a tank for future use. This method allows to eliminate the external humidifier and separate cooling plates. Comparing the phase change cooling system with the conventional water-cooling of a PEMFC it was observed that the radiator frontal area may be reduced by about 27%. The two-phase cooling system is obtained using a working fluid with a

boiling temperature within the range of the PEMFC working temperature. For instance, in case of low temperature PEMFC the working fluid with higher potential is HFE-7100, which has a boiling temperature of 61°C, while for high temperature PEMFC, which works at temperature higher than 100°C, can be use water as coolant.

3.4.2. Waste heat recovery (WHR)

The main waste heat recovery strategies developed for PEMFC systems are: to reuse the wasted heat to preheat the reactants or release hydrogen from metal hydrides (MH) tank, to exploit the wasted heat in combined heat and power (CHP) systems, to drive chillers in combined cooling and power (CCP) system, and to use heat for power generation. Since

Internal usage within the PEMFC system

Metal hydrides are particular materials that can discharge hydrogen through an endothermic reaction, named dehydrogenation. Thanks to their peculiar characteristic they are considered as promising materials for hydrogen storage for on-board hydrogen application like FCEV. Therefore it is possible to use the wasted heat from the fuel cell to heat the metal hydrides to maintain their temperature in the range of 20-30°C improving their hydrogen discharge rate. When metal hydrides (MH) are used as hydrogen storage tank, they generate cooling during hydrogen desorption and produce heat when they are absorbing hydrogen. It has been proposed a MH thermal energy storage system used to recover the wasted heat of a FCEV powertrain where the heat was reused for heating the battery at the start-up or the cabin during the drive. The results shown that the WHR recovery system proposed increases the range of the FCEV from 152 km to 178 km. Furthermore, the waste heat for MH applications can be used to preheat the reactants during operation in an extremely cold environment, instead of heat the reactants by means of electrical heater lowering the fuel cell stack output power (Baroutaji et al., 2021b).

Provide heating for combined heat power generation (CHP)

In this kind of systems PEMFC are used to produce both electrical power and heat. This system is mostly used in residential application and exploit the waste heat to increase the rooms' temperature or to obtain hot water. Thanks to the WHR the efficiency of the system increases and the energy cost and the emissions are minimized (Baroutaji et al., 2021a).

Drive chillers in combined cooling power (CCP) system

According to this WHR strategy the heat released by the PEMFC can be used for cooling purpose by driving chillers that need low temperature to operate as absorption or adsorption chillers. One possibility is to use the heat in the absorption chillers to desorb the refrigerant out of the absorbent for cooling. This system is more used with HT-PEMFCs because to drive the generator of the absorption chiller temperature up to 200 °C are more suitable. However, the feasibility of using an absorption refrigerator with a LT-PEMFC to generate both cooling and electrical power has been investigated and an increase in both maximum power density and efficiency has been reported (Baroutaji et al., 2021b).

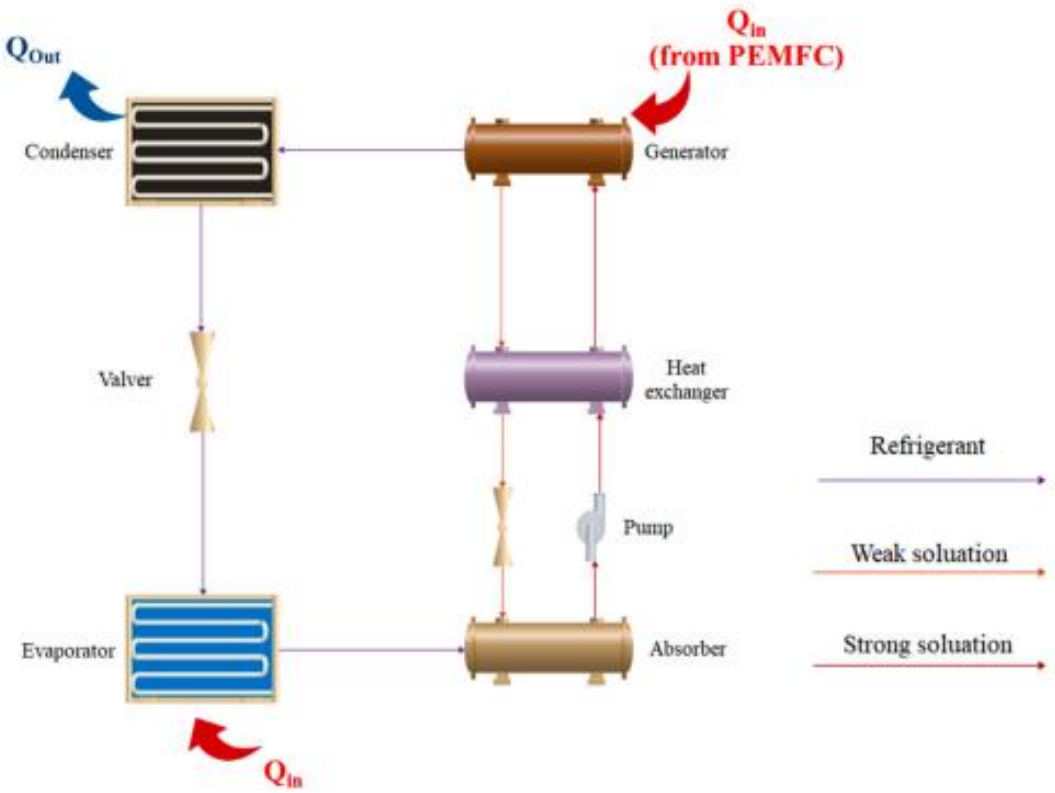

Fig. 3.12 Absorption chiller system using PEMFC waste heat to drive the generator (Baroutaji et al., 2021b)

Power generation

Finally, as mentioned before, the heat coming from the PEMFC can be exploited as heat source for thermodynamic power cycles (such as the organic Rankine cycle, ORC), creating a thermoelectric generator which is able to operate with low-grade heat sources to convert heat into electrical power. Typically, the heat produced by the fuel cell is used to heat the working fluid into the evaporator, turning it into a gaseous state to spins the turbine connected to an electrical power. According to different investigations, it was reported that the overall thermal efficiency and the power of system depend mainly on the turbine pressure ratio, type and mass flow rate of the working fluid. It was demonstrated that these systems may achieve considerable improvements in terms of power and efficiency, with increments of about 30-40%.

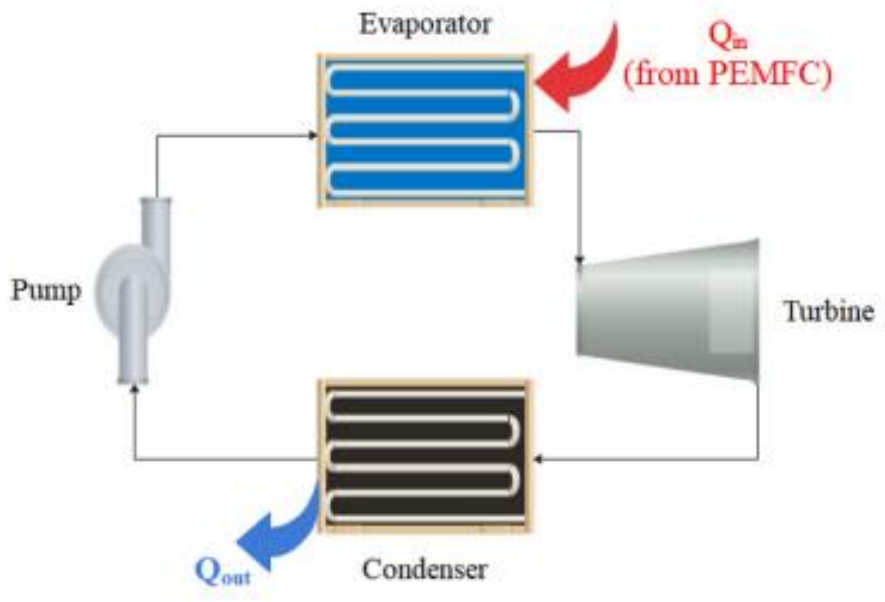

Fig. 3.13 Power generation system (Organic Rankine Cycle, ORC) using PEMFC heat in the evaporator(Baroutaji et al., 2021a)

3.5.Electrical subsystem

The electrical subsystem has to perform several tasks for the fuel cell system. It is responsible of the power delivery from the fuel cell stack to the load. In addition, it often has to modify the fuel cell electrical output characteristics (such as voltage, type of current, transient, and so on) to match the features required by the load. The electrical subsystem may either increase (so-called boost-converter) or reduce (so-called buck-converter) the fuel cell output voltage. If the load voltage is inside the fuel cell voltage range (i.e., the linear part of the fuel cell polarization curve) the electrical subsystem must be able to both work as a buck-converter and a boost-converter (Barbir, 2012).

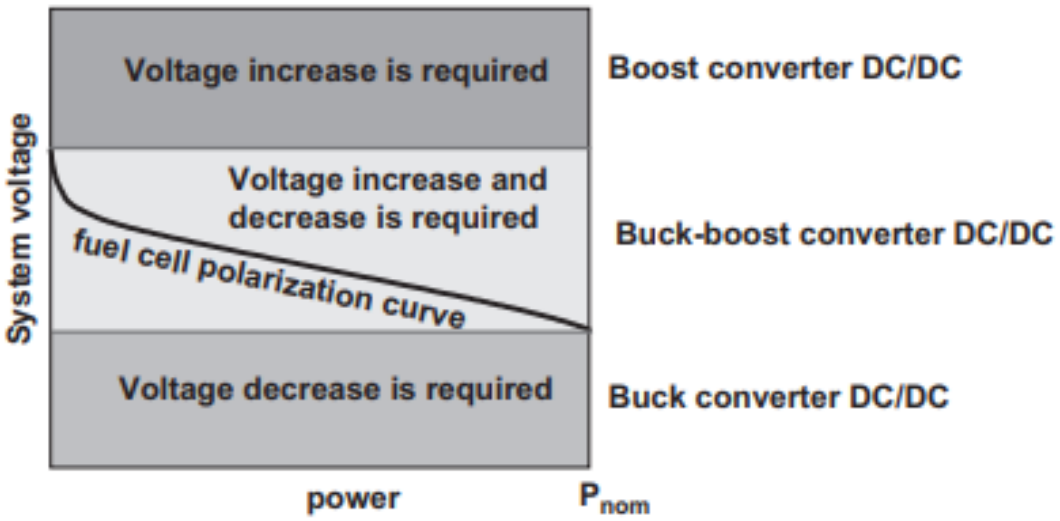

Fig. 3.14 Type of converter depending on fuel cell polarization curve (Barbir, 2012)

Voltage regulation happens through use of switching or chopping circuits that use electronic switches like:

- Thyristors and gate-turn-off (GTO) thyristors
- Metal oxide semiconductor field effect transistor (MOFSET)(low-voltage systems, up to 1kW)
- Insulated gate bipolar transistor (IGBT) for high-current applications (>50A).

Then, the output voltage is a function of input voltage (which is the fuel cell stack voltage) and the switching time. Considering a step-down, or buck-converter, the output voltage is:

$$V_{out} = DV_{in}$$

Eq. 98

Where $D = \frac{t_{on}}{t_{on}+t_{off}}$ is the switching function.

For a step-up converter, or boost-converter, the resulting output voltage is (Barbir, 2012):

$$V_{out} = \frac{V_{in}}{1 - D}$$

Eq. 99

Due to the electrical inefficiencies the actual output voltage is lower than that computed by the previous equation. Typically, the efficiency of a buck converter or a boost converter are higher than 90%, the step-down converters may reach 98% of efficiency, while the speed-up can achieve up to 95%. In case in which the load requires alternative current, AC, the electrical subsystem needs an inverter to convert direct current coming from the fuel cells to AC current at a fixed frequency (60 Hz or 50 Hz). Since the resulting inverter current is in a square-shape, in some applications the output wave required must be closer to the sinewave. In these cases, current modulation is required, and the most used method is the pulse-width modulation (PWM). The efficiency of a DC/AC inverter is in the range of 70-90%, and depends on the required power quality (Barbir, 2012).

Usually, the fuel cell systems are equipped with battery to enhance peaking power or for start up the system. When used for startup the battery has to match the voltage of the critical components to be started when the fuel cell is not operational yet. Instead, peaking batteries (or other power devices as ultracapacitors) are used to have a faster response to power changes, then they are charged by the fuel cell when its power exceeds the power request by the load. In application with high and frequent power variations, such as the automotive applications, the fuel cell is sized to provide a power level that is between the average power and peak power. So, when the power request increase, the battery covers the power difference needed. In these cases, the battery must be sized to match both the power requirements but also the energy requirements during these periods in which the fuel cell cannot recharge it (Barbir, 2012).

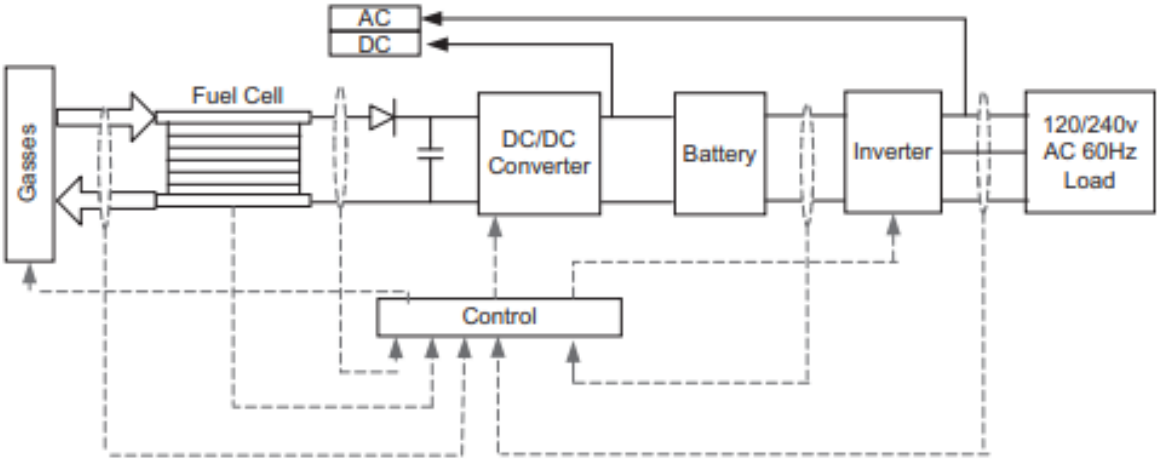

Fig. 3.15 FC electrical subsystem (Barbir, 2012)

Generally, as shown in Fig. 3.15, in a fuel cell electrical subsystem configuration the following components are present:

- A fuel cell stack (DC current)
- A buck/boost converter
- A battery or peaking device
- A diode to prevent current flow back to the fuel cell
- A capacitor just before the DC/DC converter to filter out the ripple
- A controller to ensure efficient and reliable system operation
- A power supply (DC) for auxiliary fuel cell equipment
- If the load requires AC current, an inverter (DC/AC converter) is needed.

4. Vehicle model

The objective of this master thesis is to develop a Simulink model for a hydrogen fuel cell hybrid electric heavy-duty vehicle, demonstrating the potential of this technology. This section describes the powertrain model and its characteristics. The powertrain architecture follows the design depicted in Fig. 4.1 Fuel cell electric powertrain (Hussein Basma, 2022).

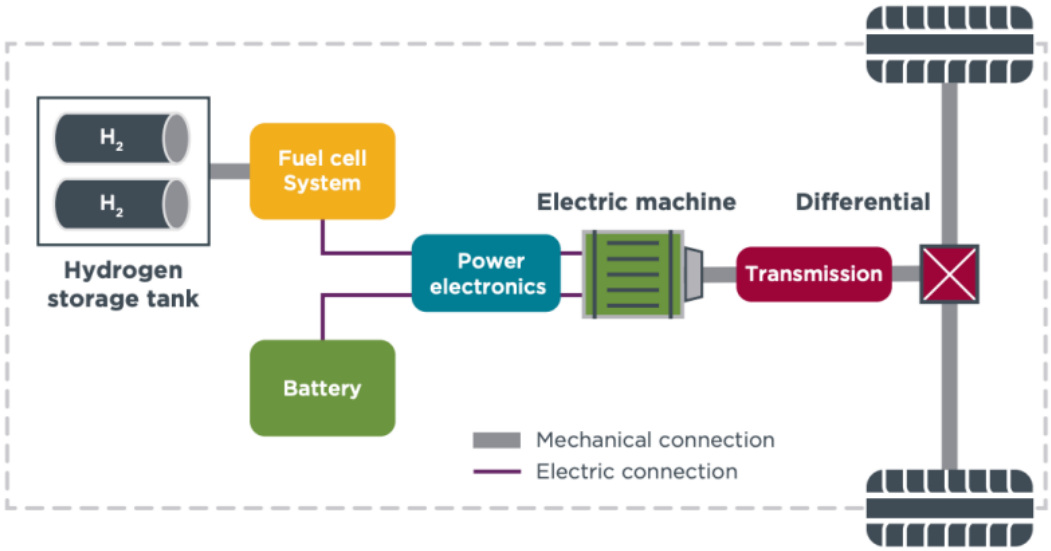

Fig. 4.1 Fuel cell electric powertrain (Hussein Basma, 2022)

4.1. Vehicle characteristics

The characteristics of the vehicle have been determined based on existing hydrogen fuel cell electric trucks, such as the aforementioned Hyundai Xcient and Iveco Nikola Tre. Fore parameters that were not available, assumptions were made considering the size and typical features of a heavy-duty vehicle.

Fig. 4.2 Hyunday Xcient (Hyundai, 2022)

4.2.Powertrain description

4.2.1. Fuel cell stack

The most suitable fuel cell type for automotive applications is the hydrogen Proton Exchange Membrane Fuel Cell (PEMFC). This technology offers excellent power density and reliability due to the absence of moving parts (Siönäs, 2022). The fuel cells and batteries are both chemical energy converters, but fuel cells have slower dynamic response due to its chemical reaction and continuous fuel supply. The fuel cell system durability is substantially dependent on the hydrogen storage capacity of the tank. Then, fuel cell stack is generally responsible for the average energy consumption and then for driving distance allowed in hybrid configuration, while the battery pack is used as power buffer. The fuel stack operating temperature is important. If its temperature exceeds a certain limit, the efficiency of the stack is reduced because of drying and, in some cases, the fuel cells can be damaged (Barbir, 2012; Siönäs, 2022). Therefore, both an energy management system and a thermal management system are necessary. Generally, the PEMFCs used for automotive applications work in a temperature range between 65 °C and 80°C, while temperature above 90°C can be dangerous for the membrane of the component.

Fig. 4.3 Hyundai Xcient FC stacks (Hyundai, 2022)

4.2.2. Battery pack

In this hybrid configuration the battery pack complements the fuel cell stack by providing a fast response to the sudden changes in power demand, improving vehicle acceleration and manoeuvrability. The battery should be designed to provide both a good peak power and, at a sufficient capacity to ensures a reasonable driving range in pure battery mode. In this way, the fuel cell stack can operate near its nominal conditions, where its efficiency is higher. Unlike the fuel cell stack, which can only generate current consuming hydrogen and oxygen, the battery can both discharge and charge, allowing the regenerative braking, recovering part of the energy during deceleration, and improving the overall efficiency of the vehicle. Being a chemical energy converter, also the battery's temperature needs to be maintained in a certain range (usually between 0°C and 40°C) (Barbir, 2012; Siönäs, 2022). Nevertheless, the operating temperature of the battery is lower than the fuel cell one, so it is more difficult to be manged.

4.2.3. Electric machine

The electric machine converts the electric power generated by fuel cell stack and/or battery pack into mechanical energy necessary to propel the vehicle. During the braking process, the machine generates current for recharging battery. For heavy-duty applications, AC machine are commonly used to their higher efficiency; simpler construction; reliability (they have fewer components and don't require brushes and commutators, which are common wear items in DC machines). The Hyundai Xcient and the Nikola Tre, for instance, mounts a PM-SyR (permanent magnets assisted synchronous reluctance machine) and a PMSM (permanent magnets synchronous machine), respectively. Both machines offer high levels of efficiency and high torque density. The difference between them is that the PM-SyR more cost-effective because of the use of smaller magnets, while the PMSM is easier to control.

4.2.4. Power electronics

The power electronics plays a crucial role in voltage and current modulation in order to connect components with different voltages, such as DC-DC converters, and facilitates the connection between a DC power source and an AC load. For this hybrid heavy-duty vehicle configuration, at least three DC-DC converters are required: one for the connection between battery and FC stack, and two for the low voltage connections of the auxiliaries. Moreover, an inverter is needed to convert the DC voltage into AC electric signal for the AC traction motor, the maximum IGBT voltage of the inverter must be $\frac{3}{2}$ times higher than the maximum DC BUS voltage.

4.2.5. Gear transmission

The vehicle transmission is generally composed by the gear box and the differential. In this case, considering that the vehicle uses an electric motor, the gear box step can be avoided. In some cases, according to the torque and speed required by the different working condition, one (e.g. when the overall gear ratio needed is higher than the maximum gear ratio of the differential) or two different gear ratios can be designed (e.g., when steep climb are expected in the vehicle driving mission, to have a better modulation of the torque). But these solutions obviously have a higher cost and lead to a farther increase in transmission weight.

5. Simulink model

To develop a model through which explore the different ways to exploit the characteristics of the system the MATLAB/Simulink environment have been chosen. The model is divided into three areas:

- the vehicle dynamic
- the power supply system
- the measurements.

In the vehicle dynamic part is used to quantify the current required by the electric machine to propel a vehicle during a driving cycle, while the power supply model simulate the behaviour of the FC stack and battery subjected to the same mission. In the Fig. 5.1 FC hybrid heavy-duty vehicle modelFig. 5.1 the developed Simulink model is presented.

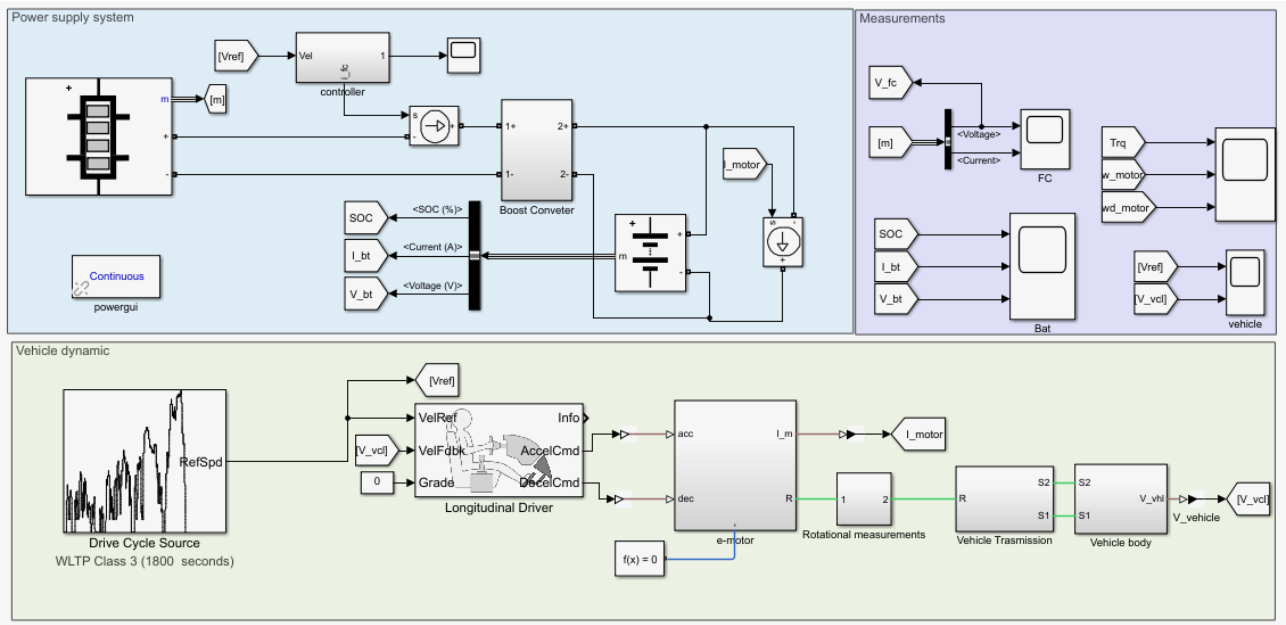

Fig. 5.1 FC hybrid heavy-duty vehicle model

The following sections present a model for each part of the overall vehicle model. The model assumptions are:

- A quasi-static model is used.
- No nitrogen is diffused through the membrane.
- The output voltage is only affected by the activation
- The output voltage is only affected by the activation-, ohmic- and concentrationlosses. All useful output voltage can produce work in the powertrain
- Ideal temperature distribution in the FC stack.
- The power consumed by hydrogen- and water-circuit are neglected
- The process of turning the FC on and off does not waste any extra hydrogen.
- No thermal effects on the components are considered

- The efficiencies of the components are considered constant
- Fuel consumption are not considered.

5.1.Vehicle dynamic

This vehicle dynamic model simulates a vehicle driven by a driver which follows a specific driving cycle.

It is composed by:

- Driving cycle and longitudinal driver
- Electric machine
- Vehicle transmission
- Vehicle body

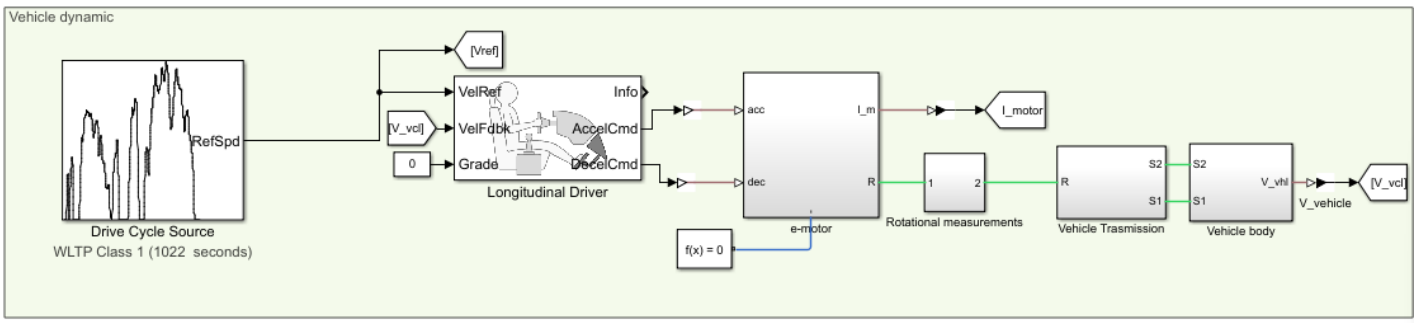

- *Fig. 5.2 Vehicle dynamic model*

5.1.1. Driving cycle and longitudinal driver

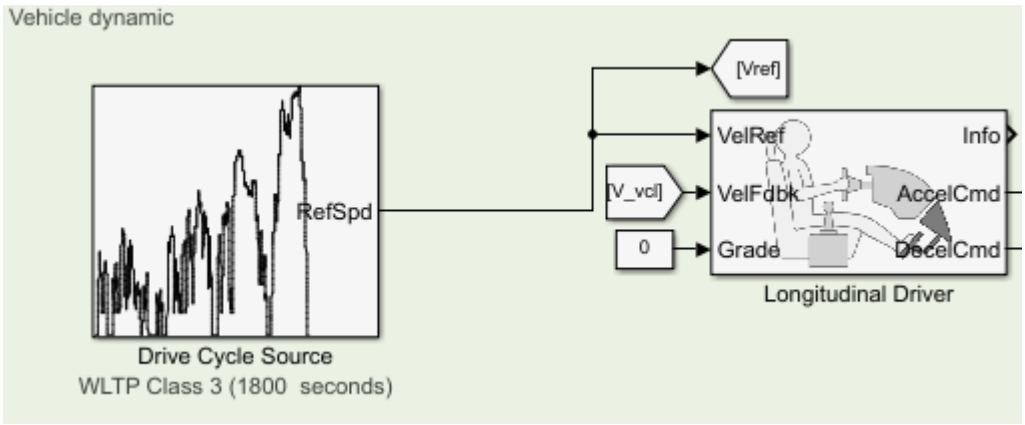

Fig. 5.3 Driving cycle source and Longitudinal driver

These two blocs determine the acceleration and deceleration requested to the electric motor. The driving cycle source block allows to choose between different velocity profiles. For the objective of this thesis the WLTP 1 have been selected because is a trade of between the sever speed profile and acceptable computational time.

The Longitudinal driver emulate the acceleration (and deceleration) action of the driver. It compares the reference velocity, which is the speed profile of the driving cycle, to the feedback actual vehicle velocity, and through a PI controller it computes the accelerating or decelerating command.

5.1.2. Electric machine

Being the object of this thesis focused on the behaviour of the FC stack, a simple DC motor have been chosen because it is easier to be modelled and to reduce the computation time of the simulation. It converts the electric power requested by the driver through the PWM into the mechanical power needed to propel the vehicle.

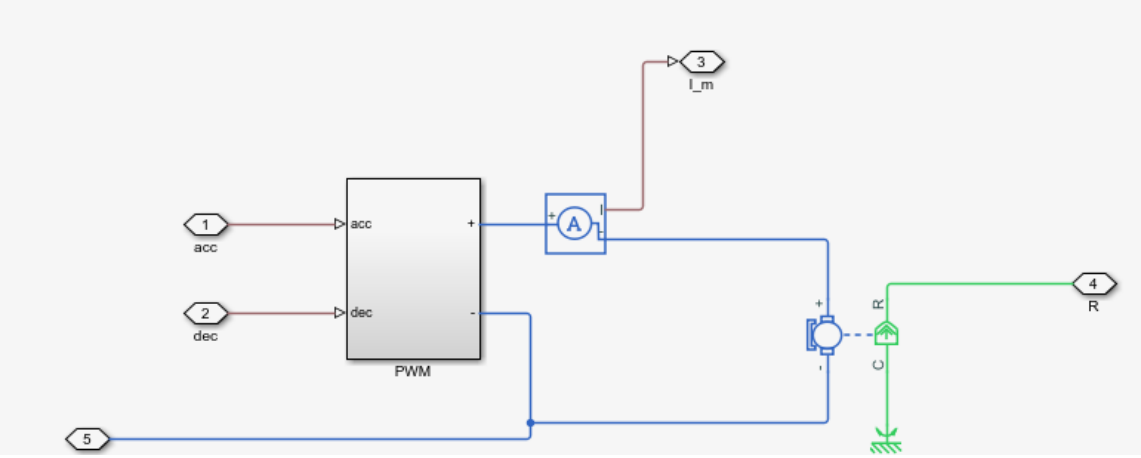

Fig. 5.4 DC motor and PWM controller

Motor characteristics are listed in the table below.

Table 5 DC motor model parameters

Field type	**Permanent magnet**
Armature inductance	$12\ \mu H$
Stall torque	$3500\ Nm$
No-load speed	$7500\ rpm$
Rated DC supply voltage	$720\ V$
Rotor inertia	$1.2\ kgm^2$

The acceleration and deceleration command obtained from the longitudinal driver block are voltage inputs that are converted into a PWM signal to control the DC motor. The PWM controller scheme is presented in Fig. 5.5

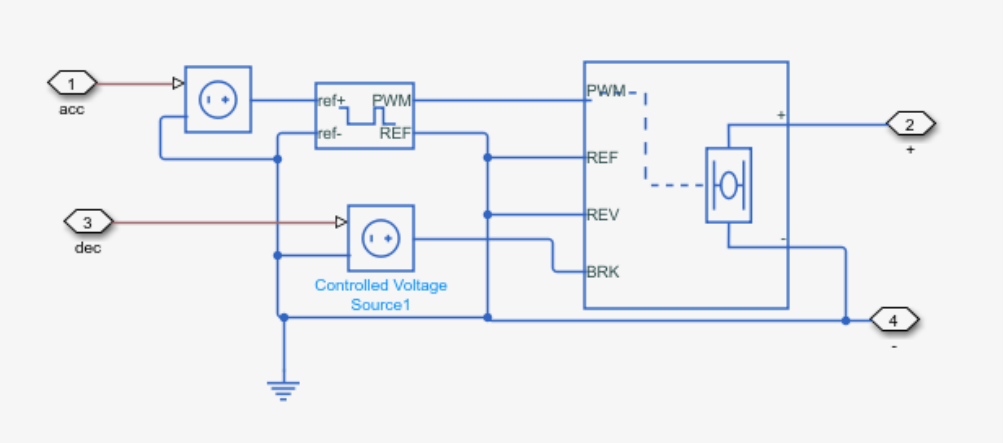

Fig. 5.5 PWM controller model

5.1.3. Gear transmission

As shown in Fig. 5.6 the vehicle transmission is simply composed by a simple gear coupling and a epicyclical differential.

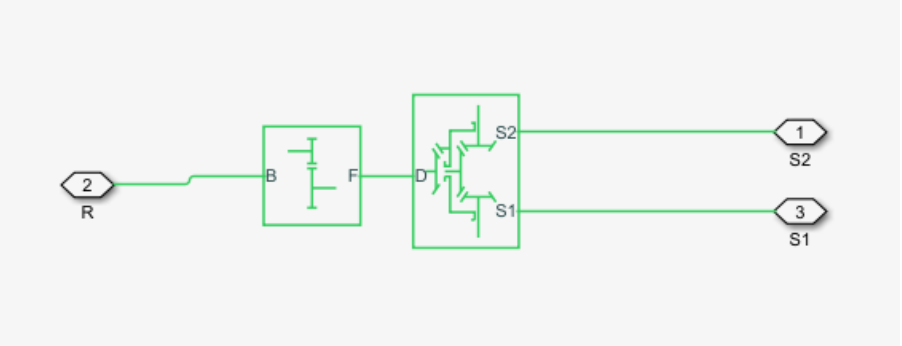

Fig. 5.6 simple gear and differential

The simple gear has a unitary gear ratio. Since the gear ratio is equal to unit, it can be avoided, nevertheless it was added to the model because in several cases a gear coupling is needed to solve layout issues.

The differential, instead, has a total gear ratio $\tau_{diff} = 5.73$. The gear ratio is modelled considering a maximum vehicle speed of 150 km/h. In Table 6 below the transmission parameter used are reported.

Table 6 Transmission parameters

Transmission parameters	$\boldsymbol{gear\ ratio}$	efficiency
Simple gear	1	0.97
Epicycloid differential	5.73	[0.82 0.90]

5.1.4. Vehicle body

At the end of the vehicle model there is the vehicle body block which is connected to the tires. In this configuration, a rear-wheel-drive configuration is used. Given that the lateral dynamic of the

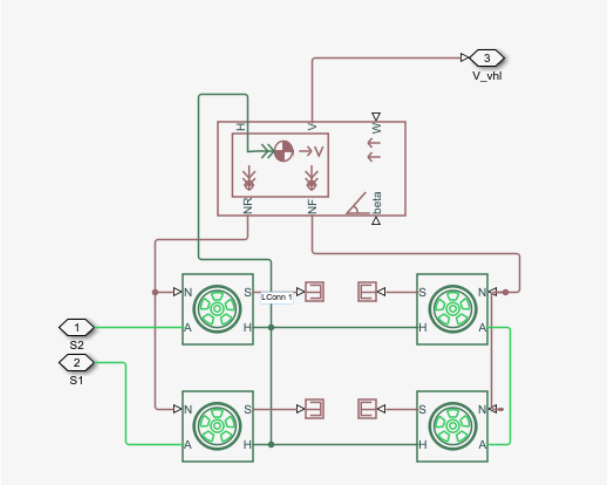

Fig. 5.7 Vehicle body and tire block

vehicle is not considered, the different wheel drive possible configurations are not significant for this analysis.

The block of the tires is used to compute the vehicle speed, by means of the rolling radius, and the rolling resistance through the tire magic formula. In table x both the vehicle and tires parameters are listed.

Vehicle mass empty	$\boldsymbol{m_{vehicle}}$	$\mathbf{9500\ kg}$
Vehicle mass full load	m_{full}	$30000\ kg$
Vehicle frontal area	$A_{frontal}$	$8\ m^2$
Aerodynamic drag coefficient	C_x	0.45-
Rolling resistance coefficient	f_{roll}	0.008
Tire radius	r_{tire}	$0.506\ m$

5.2. Power supply model

The power supply system is composed by: FC stack block, boost DC converter, battery. The system is loaded by means of a controlled current source which impose the current requested by the DC motor. Moreover, to consider the efficiency of the inverter which should be used in a real configuration, the current is roughly divided by the hypothesized inverter efficiency. In fig x there is a representation of the Simulink model.

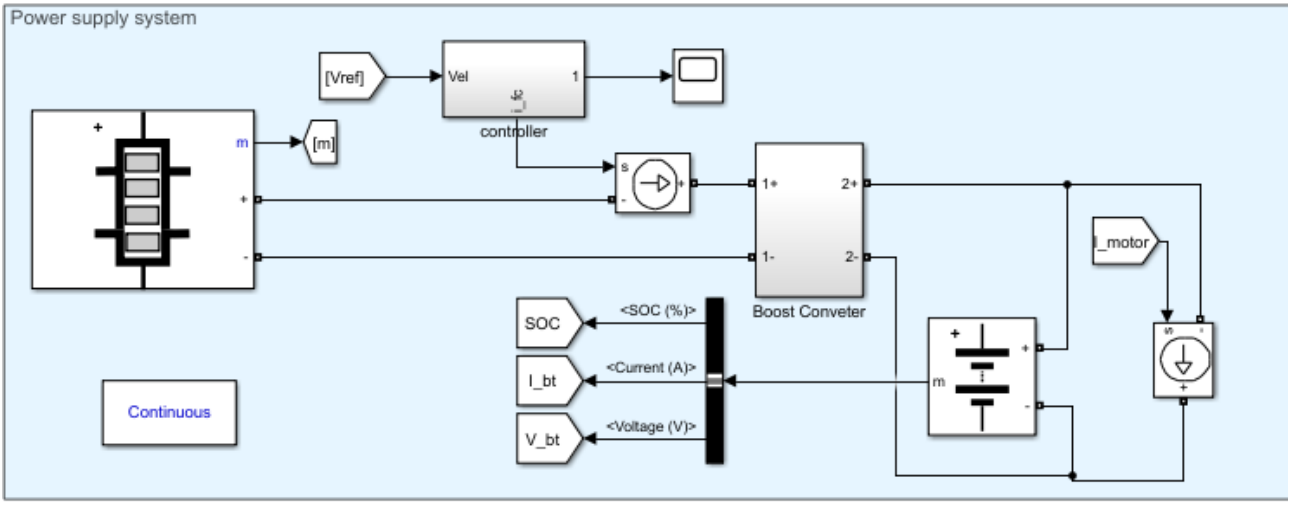

Fig. 5.8 Power supply system model

5.2.1. Fuel cell stack and Boost DC converter

MATLAB/Simulink environment provides a parametrized block which works as PEMFC stack. Modifying the several parameters it is possible to model the FC stack with the polarization curve desired. The parameters of the fuel cell stack, which are listed in tab x, have been set taking as example the Hyundai Xcient fuel cell truck, which is equipped with two FC stack with a total power of 180 kW.

Table 7 FC stack parameters

Voltage at 0 A and 1 A	[650 V, 635 V]
Nominal operating point	$[\,350\ A, 500\ V]$
Maximum operating point	$[900\ A, 400\ V$
Number of cells	650
Nominal stack efficiency	0.55
Operating temperature	$75\ °C$

The FC stack is designed to work about at its nominal conditions because of its efficiency, which decreases increasing the current, then also with increasing power. The designed FC stack polarization and power curves result to be like in figure.

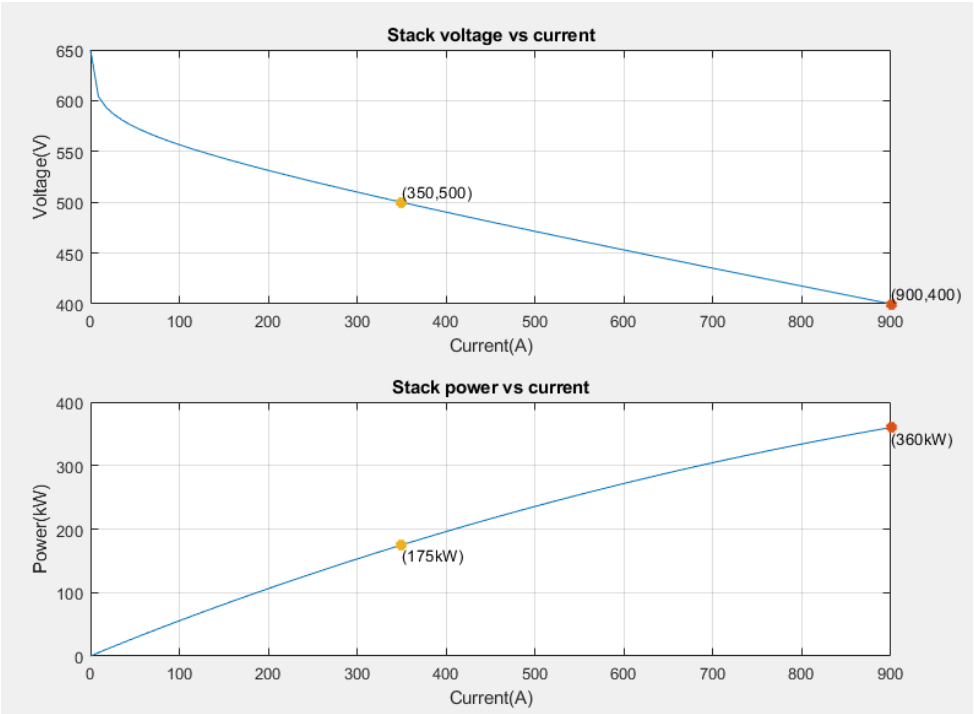

Fig. 5.9 Polarization curve and power curve of the FC stack

To connect the FC stack with the high voltage battery a simple boost DC converter have been developed. The d block is the duty cycle imposed to the MOSFET.

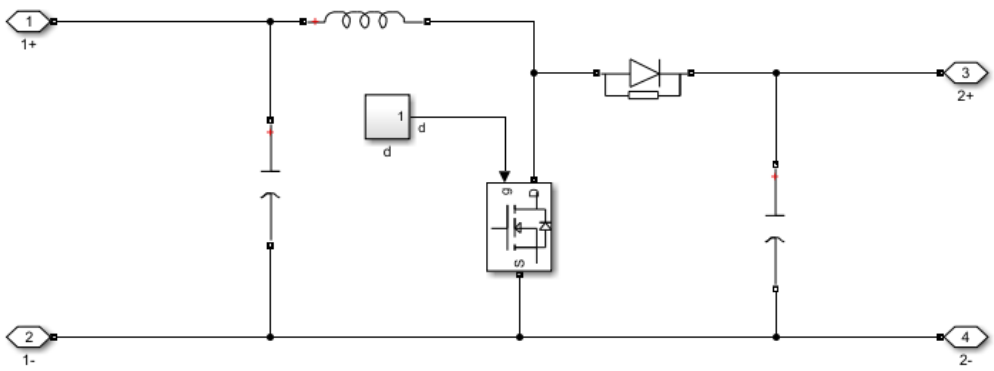

Fig. 5.10 Boost DC converter

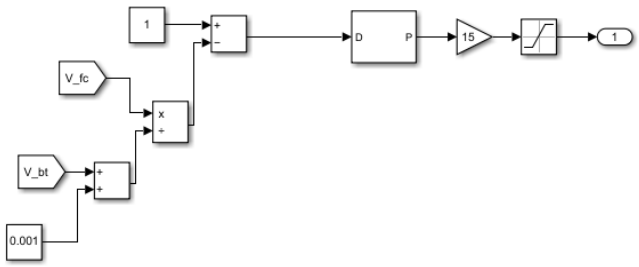

Fig. 5.11 MOSFET duty cycle

5.2.2. Battery

The battery has been designed taking as reference the battery of the Xcient. The MATLAB/Simulink environment propose several possibilities to model a battery. The model chosen implements a generic battery for most popular types.

Nominal voltage	**720**
Rated capacity	200 Ah
Battery response time	30 s

Bibliography

» Hyundai e H2Energy insieme per una spinta alla mobilità idrogeno in Europa. (n.d.). Retrieved February 28, 2023, from https://www.h2it.it/hyundai-e-h2energy-insieme-per-una-spinta-alla-mobilita-idrogeno-in-europa/

2 Typical polarization curve of a PEM fuel cell. | Download Scientific Diagram. (n.d.). Retrieved February 28, 2023, from https://www.researchgate.net/figure/Typical-polarization-curve-of-a-PEM-fuel-cell_fig2_314087767

2021 Clarity Fuel Cell Specifications & Features. (n.d.). Retrieved February 27, 2023, from https://hondanews.com/en-US/honda-automobiles/releases/release-4f88c507e72a4e7630685979cb04f2cb-2021-clarity-fuel-cell-specifications-features

2023 Toyota Mirai | Toyota.com. (n.d.). Retrieved February 27, 2023, from https://www.toyota.com/mirai/

About the Fuel Cell Power Chevy Colorado ZH2| Wright Chevy Buick GMC. (n.d.). Retrieved February 26, 2023, from https://www.wrightchevroletbuickgmc.com/chevy-colorado-zh2-blog#close

Alstom's Coradia iLint hydrogen train runs for the first time in France | Alstom. (n.d.). Retrieved February 26, 2023, from https://www.alstom.com/press-releases-news/2021/9/alstoms-coradia-ilint-hydrogen-train-runs-first-time-france

Alstom Coradia-LINT - Wikipedia. (n.d.). Retrieved February 28, 2023, from https://it.wikipedia.org/wiki/Alstom_Coradia-LINT

Alstom Coradia iLint. (n.d.). Retrieved February 28, 2023, from https://www.alstom.com/solutions/rolling-stock/alstom-coradia-ilint-worlds-1st-hydrogen-powered-train

Alstom unveils hydrogen fuel cell regional train Coradia iLint - Green Car Congress. (n.d.). Retrieved February 26, 2023, from https://www.greencarcongress.com/2016/09/alstom-unveils-hydrogen-fuel-cell-regional-train-coradia-ilint.html

Barbir, F. (2012). Fuel Cell Modeling. In *PEM Fuel Cells: Theory and Practice* (Issue Dc). https://doi.org/10.1016/B978-0-12-387710-9.00009-6

Baroutaji, A., Arjunan, A., Ramadan, M., Robinson, J., Alaswad, A., Abdelkareem, M. A., & Olabi, A.-G. (2021a). *Advancements and prospects of thermal management and waste heat recovery of PEMFC*. https://doi.org/10.1016/j.ijft.2021.100064

Baroutaji, A., Arjunan, A., Ramadan, M., Robinson, J., Alaswad, A., Abdelkareem, M. A., & Olabi, A. G. (2021b). Advancements and prospects of thermal management and waste heat recovery of PEMFC. *International Journal of Thermofluids*, *9*, 100064. https://doi.org/10.1016/j.ijft.2021.100064

BHD., W. A. S. (2023). *Honda FCX Clarity 2008 car price, specs, images, installment schedule, review | Wapcar.my*. https://www.wapcar.my/previous-cars/honda/honda-fcx-clarity-2008

Bonci, M. (2021). *Master degree thesis Fuel Cell Vehicle simulation : an approach based on Toyota Mirai*. 0–106.

CNH Industrial's Iveco unveils first electric truck in partnership with Nikola | Reuters. (n.d.). Retrieved February 27, 2023, from https://www.reuters.com/article/us-cnh-industrial-nikola-idUSKBN1Y62FR

CO_2 emission performance standards for cars and vans. (n.d.). Retrieved February 27, 2023, from https://climate.ec.europa.eu/eu-action/transport-emissions/road-transport-reducing-co2-emissions-vehicles/co2-emission-performance-standards-cars-and-vans_en

Daimler and Shell Team up on Hydrogen Trucks. (n.d.). Retrieved February 28, 2023, from https://www.autoweek.com/news/green-cars/a36519435/daimler-and-shell-hydrogen-trucks/

Daimler plans H2 truck with 1,000 km range - electrive.com. (n.d.). Retrieved February 28, 2023, from https://www.electrive.com/2020/09/16/daimler-reveals-plans-for-fuel-cell-truck-with-1000-km-range/

DeCicco, J. M. (2004). The "Chicken or Egg" Problem Writ Large: Why a Hydrogen Fuel Cell Focus Is Premature. *The Hydrogen Energy Transition: Cutting Carbon from Transportation*, 213–226. https://doi.org/10.1016/B978-012656881-3/50015-0

Development milestone: Daimler Truck tests fuel-cell truck with liquid hydrogen - Daimler Truck Media Site. (n.d.). Retrieved February 27, 2023, from https://media.daimlertruck.com/marsMediaSite/en/instance/ko/Development-milestone-Daimler-Truck-tests-fuel-cell-truck-with-liquid-hydrogen.xhtml?oid=51975637

Engineering the Extreme Capability of the Colorado ZH2. (n.d.). Retrieved February 28, 2023, from https://media.chevrolet.com/media/us/en/chevrolet/home.detail.html/content/Pages/news/us/en/2016/oct/1101-zh2.html

Executive summary – Global Hydrogen Review 2022 – Analysis - IEA. (n.d.). Retrieved February 28, 2023, from https://www.iea.org/reports/global-hydrogen-review-2022/executive-summary

Fuel-Cell Mercedes-Benz GenH2 Truck Passes Challenging Tests With Flying Colors - autoevolution. (n.d.). Retrieved February 26, 2023, from https://www.autoevolution.com/news/fuel-cell-mercedes-benz-genh2-truck-passes-challenging-tests-with-flying-colors-161630.html

Fuel cell bus - Wikipedia. (n.d.). Retrieved February 28, 2023, from https://en.wikipedia.org/wiki/Fuel_cell_bus

Fuel cell voltage and voltage losses as a function of current density... | Download Scientific Diagram. (n.d.). Retrieved February 28, 2023, from https://www.researchgate.net/figure/Fuel-cell-voltage-and-voltage-losses-as-a-function-of-current-density-at-3-atm_fig3_334468259

Honda Clarity - Wikipedia. (n.d.). Retrieved February 28, 2023, from https://en.wikipedia.org/wiki/Honda_Clarity

Honda Clarity Fuel Cell vanta un'autonomia di 589 km certificata EPA. (n.d.). Retrieved February 27, 2023, from https://www.honda.it/cars/world-of-honda/present/news-events/honda-clarity-fuel-cell-vanta-unautonomia-di-589-km-certificata-.html

Hopium, Manufacturer Of High-end Hydrogen Powered Vehicles, Unveils The Hopium Machina Vision and Announces The Opening of its Order Book - Hydrogen Central. (n.d.). Retrieved February 27, 2023, from https://hydrogen-central.com/hopium-manufacturer-high-hydrogen-powered-vehicles-unveils-hopium-machina-vision-announces-opening-order-book/

Hopium - Wikipedia. (n.d.). Retrieved February 28, 2023, from https://en.wikipedia.org/wiki/Hopium

Hopium Machina Alpha 0 Hits the Road! (n.d.). Retrieved February 28, 2023, from https://www.finyear.com/Hopium-Machina-Alpha-0-Hits-the-Road_a44792.html?com

Hopium Machina Technology. (n.d.). Retrieved February 27, 2023, from https://hopium.com/technology/

How Fuel Cells Work. (n.d.). Retrieved March 4, 2023, from https://www.fueleconomy.gov/feg/fcv_pem.shtml

Hydrail - Wikipedia. (n.d.). Retrieved February 27, 2023, from https://en.wikipedia.org/wiki/Hydrail

Hydrogen-fuelled tractors: a clean energy option for farmers. (n.d.). Retrieved February 28, 2023, from https://www.nswfarmers.org.au/NSWFA/Posts/The_Farmer/Tools/Hydrogen_fuelled_tractors_a_clea

n_energy_option_for_farmers.aspx

Hydrogen trains coming soon? - Rail Engineer. (n.d.). Retrieved February 28, 2023, from https://www.railengineer.co.uk/hydrogen-trains-coming-soon/

Hyundai. (2022). *XCIENT Fuel Cell Brochure*. https://truckbus.hyundai.com/global/en/products/truck/xcient-fuel-cell

Hyundai e H2 Energy: nuova joint venture per spingere la mobilità a idrogeno in Europa. (n.d.). Retrieved February 28, 2023, from https://www.hyundai.news/it/articles/press-releases/hyundai-e-h2-energy-nuova-joint-venture-per-spingere-la-mobilita-a-idrogeno-in-europa.html

Hyundai Fuel Cell Truck & Bus | Hydrogen-powered, zero-emission car. (n.d.). Retrieved February 27, 2023, from https://trucknbus.hyundai.com/hydrogen/en

Hyundai goes full steam ahead on fuel cell systems - electrive.com. (n.d.). Retrieved February 26, 2023, from https://www.electrive.com/2018/12/11/hyundai-goes-full-steam-ahead-on-fuel-cell-systems/

Hyundai ix35 FCEV - Wikipedia. (n.d.). Retrieved February 27, 2023, from https://en.wikipedia.org/wiki/Hyundai_ix35_FCEV

Hyundai ix35 Fuel Cell 2013-2018 Review (2023) | Autocar. (n.d.). Retrieved February 26, 2023, from https://www.autocar.co.uk/car-review/hyundai/ix35-fuel-cell-2013-2018

Hyundai Nexo, la sicurezza dell'idrogeno - Motori. (n.d.). Retrieved February 28, 2023, from https://motori.ilgiornale.it/hyundai-nexo-la-sicurezza-dellidrogeno/

Hyundai Nexo - Wikipedia. (n.d.). Retrieved February 27, 2023, from https://en.wikipedia.org/wiki/Hyundai_Nexo

Iveco presents new BEV & FCEV vans and trucks with Hyundai & Nikola Motor - electrive.com. (n.d.). Retrieved February 28, 2023, from https://www.electrive.com/2022/09/19/iveco-presents-new-bev-fcev-vans-and-trucks-with-hyundai-nikola-motor/

JCB's First Hydrogen Powered Excavator | News | JCB.com. (n.d.). Retrieved February 27, 2023, from https://www.jcb.com/en-gb/news/2020/07/jcb-leads-the-way-with-first-hydrogen-fuelled-excavator

Kramer, D. (2017). Hydrogen-powered vehicles: A chicken and egg problem. *Physics Today*, *70*(9), 31. https://doi.org/10.1063/PT.3.3690

La Normandie ne veut pas perdre sa marque automobile Hopium. (n.d.). Retrieved February 28, 2023, from https://www.presse-citron.net/la-normandie-ne-veut-pas-perdre-sa-marque-automobile-hopium/

LCA | 2nd generation Toyota Mirai | Toyota Europe. (n.d.). Retrieved February 26, 2023, from https://www.toyota-europe.com/sustainability/carbon-neutrality/vehicle-life-cycle-assessments/lca-2nd-generation-mirai

Liso, V., & Araya, S. S. (2021). Thermodynamics and operating conditions for proton exchange membrane fuel cells. In *PEM Fuel Cells: Fundamentals, Advanced Technologies, and Practical Application*. INC. https://doi.org/10.1016/B978-0-12-823708-3.00014-6

Mission-Ready Chevrolet Colorado ZH2 Fuel Cell Vehicle Breaks Cover at U.S. Army Show. (n.d.). Retrieved February 28, 2023, from https://news.gm.com/newsroom.detail.html/Pages/news/us/en/2016/oct/1003-zh2.html

Nanaki, E. A., Koroneos, C. J., Roset, J., Susca, T., Christensen, T. H., De Gregorio Hurtado, S., Rybka, A., Kopitovic, J., Heidrich, O., & López-Jiménez, P. A. (2017). Environmental assessment of 9 European public bus transportation systems. *Sustainable Cities and Society*, *28*, 42–52. https://doi.org/10.1016/J.SCS.2016.08.025

New Holland's NH2 Hydrogen Fuel cell tractor. (n.d.). Retrieved February 26, 2023, from https://newatlas.com/new-holland-nh2-hydrogen-powered-tractor/11171/

New Holland NH2 Hydrogen Tractor | Inhabitat - Green Design, Innovation, Architecture, Green Building. (n.d.). Retrieved February 26, 2023, from https://inhabitat.com/new-holland-unveils-nh2-hydrogen-fuel-cell-tractor-for-greening-farm-work/rsz-new-holland-nh2-hydrogen-tractor-1/

New Holland presents the first NH2^{TM} hydrogen powered tractor ready to go into service on a farm | NHAG. (n.d.). Retrieved February 27, 2023, from https://agriculture.newholland.com/eu/en-uk/about-us/whats-on/news-events/2011/nh2

New Mirai hydrogen fuel cell electric vehicle - under the skin - Toyota UK Magazine. (n.d.). Retrieved February 28, 2023, from https://mag.toyota.co.uk/new-mirai-hydrogen-fuel-cell-electric-vehicle/

NEXO | Dimensioni, prezzo, listino e scheda tecnica | Hyundai. (n.d.). Retrieved February 27, 2023, from https://www.hyundai.com/it/models/nexo/listino-e-scheda-tecnica.html

Nikola to utilize fuel-cell power modules using technology licensed from Bosch - Green Car Congress. (n.d.). Retrieved February 26, 2023, from https://www.greencarcongress.com/2021/09/20210903-nikola.html

Paris Agreement. (n.d.). Retrieved February 27, 2023, from https://climate.ec.europa.eu/eu-action/international-action-climate-change/climate-negotiations/paris-agreement_en

Qureshi, F., Yusuf, M., Kamyab, H., Vo, D. V. N., Chelliapan, S., Joo, S. W., & Vasseghian, Y. (2022). Latest eco-friendly avenues on hydrogen production towards a circular bioeconomy: Currents challenges, innovative insights, and future perspectives. *Renewable and Sustainable Energy Reviews*, *168*, 112916. https://doi.org/10.1016/J.RSER.2022.112916

Review, Jadwal angsuran, Spek, Gambar, Harga Honda FCX Clarity 2007 | Autofun. (n.d.). Retrieved February 28, 2023, from https://www.autofun.co.id/previous-mobil/honda/honda-fcx-clarity-2007

Schäfer, A., Heywood, J. B., & Weiss, M. A. (2006). Future fuel cell and internal combustion engine automobile technologies: A 25-year life cycle and fleet impact assessment. *Energy*, *31*(12), 2064–2087. https://doi.org/10.1016/J.ENERGY.2005.09.011

Selmi, T., Khadhraoui, A., & Cherif, A. (2022). Fuel cell–based electric vehicles technologies and challenges. *Environmental Science and Pollution Research*, *29*(52), 78121–78131. https://doi.org/10.1007/S11356-022-23171-W/FIGURES/7

Shabani, B., & Andrews, J. (2015). Hydrogen and fuel cells. *Green Energy and Technology*, *201*, 453–491. https://doi.org/10.1007/978-81-322-2337-5_17/FIGURES/20

Sharma, P., & Pandey, O. P. (2021). Proton exchange membrane fuel cells: Fundamentals, advanced technologies, and practical applications. *PEM Fuel Cells: Fundamentals, Advanced Technologies, and Practical Application*, 1–24. https://doi.org/10.1016/B978-0-12-823708-3.00006-7

Singla, M. K., Nijhawan, P., & Oberoi, A. S. (2021). Hydrogen fuel and fuel cell technology for cleaner future: a review. *Environmental Science and Pollution Research 2021 28:13*, *28*(13), 15607–15626. https://doi.org/10.1007/S11356-020-12231-8

Siönäs, D. S. & J. (2022). Optimal Control and Thermal Management of Heavy-Duty FCHEV Powertrains. *Master, Electrical Engineering Systems, Vehicular*, 13–28.

Staffell, I., Scamman, D., Velazquez Abad, A., Balcombe, P., Dodds, P. E., Ekins, P., Shah, N., & Ward, K. R. (2019). The role of hydrogen and fuel cells in the global energy system. *Energy & Environmental Science*, *12*(2), 463–491. https://doi.org/10.1039/C8EE01157E

Sutharssan, T., Montalvão, D., Chen, Y., Wang, W.-C., Pisac, C., & Elemara, H. (2016). A review on

prognostics and health monitoring of proton exchange membrane fuel cell. *Renewable and Sustainable Energy Reviews*, *75*. https://doi.org/10.1016/j.rser.2016.11.009

Toyota. (2014). Outline of the Mirai Key Specifications. *Toyota Motor Corporation*, *November*, 13. http://newsroom.toyota.co.jp/en/download/4224903

Toyota Fuel Cell Applications | Toyota Europe. (n.d.). Retrieved February 28, 2023, from https://www.toyota-europe.com/brands-and-services/toyota-fuel-cell/fuel-cell-applications

Toyota Fuel Cell Electric Vehicles | Toyota Europe. (n.d.). Retrieved February 28, 2023, from https://www.toyota-europe.com/electrification/fcev

Toyota Mirai - Wikipedia. (n.d.). Retrieved February 27, 2023, from https://en.wikipedia.org/wiki/Toyota_Mirai

Toyota Mirai Hydrogen Fuel Cell. (n.d.). Retrieved February 28, 2023, from https://www.glpautogas.info/en/toyota-mirai-hydrogen.html

TOYOTA PRESENTA IL PROTOTIPO "SORA", L'AUTOBUS EQUIPAGGIATO CON CELLE A COMBUSTIBILE. (n.d.). Retrieved February 28, 2023, from https://newsroom.toyota.it/toyota-presenta-il-prototipo-sora/

Toyota ramps up efforts to look at potential of hydrogen vehicles. (n.d.). Retrieved February 26, 2023, from https://www.cnbc.com/2022/05/18/toyota-ramps-up-efforts-to-look-at-potential-of-hydrogen-vehicles.html

Toyota Sora - Wikipedia. (n.d.). Retrieved February 28, 2023, from https://en.wikipedia.org/wiki/Toyota_Sora

Toyota Sora Fuel Cell bus gets more safety and communication tech - Autodevot. (n.d.). Retrieved February 26, 2023, from https://www.autodevot.com/2019/08/toyota-sora-fuel-cell-bus-gets-more-safety-tech/

Tre FCEV: Fuel-Cell Electric Metro-Regional Semi-Truck. (n.d.). Retrieved February 27, 2023, from https://nikolamotor.com/tre-fcev

Usmanov, U. (2022). *Mirai based fuel cell hybrid electric vehicles* (Issue June).

XCIENT Fuel Cell | HYUNDAI Truck & Bus. (n.d.). Retrieved February 27, 2023, from https://trucknbus.hyundai.com/global/en/products/truck/xcient-fuel-cell

Yuan, Y., Qu, Z., Wang, W., Ren, G., & Hu, B. (2019). Illustrative Case Study on the Performance and Optimization of Proton Exchange Membrane Fuel Cell. *ChemEngineering 2019, Vol. 3, Page 23*, *3*(1), 23. https://doi.org/10.3390/CHEMENGINEERING3010023

Yusuf, M., Alnarabiji, M. S., & Abdullah, B. (2021). Clean Hydrogen Production Technologies. *Advances in Sustainable Energy*, 159–170. https://doi.org/10.1007/978-3-030-74406-9_5